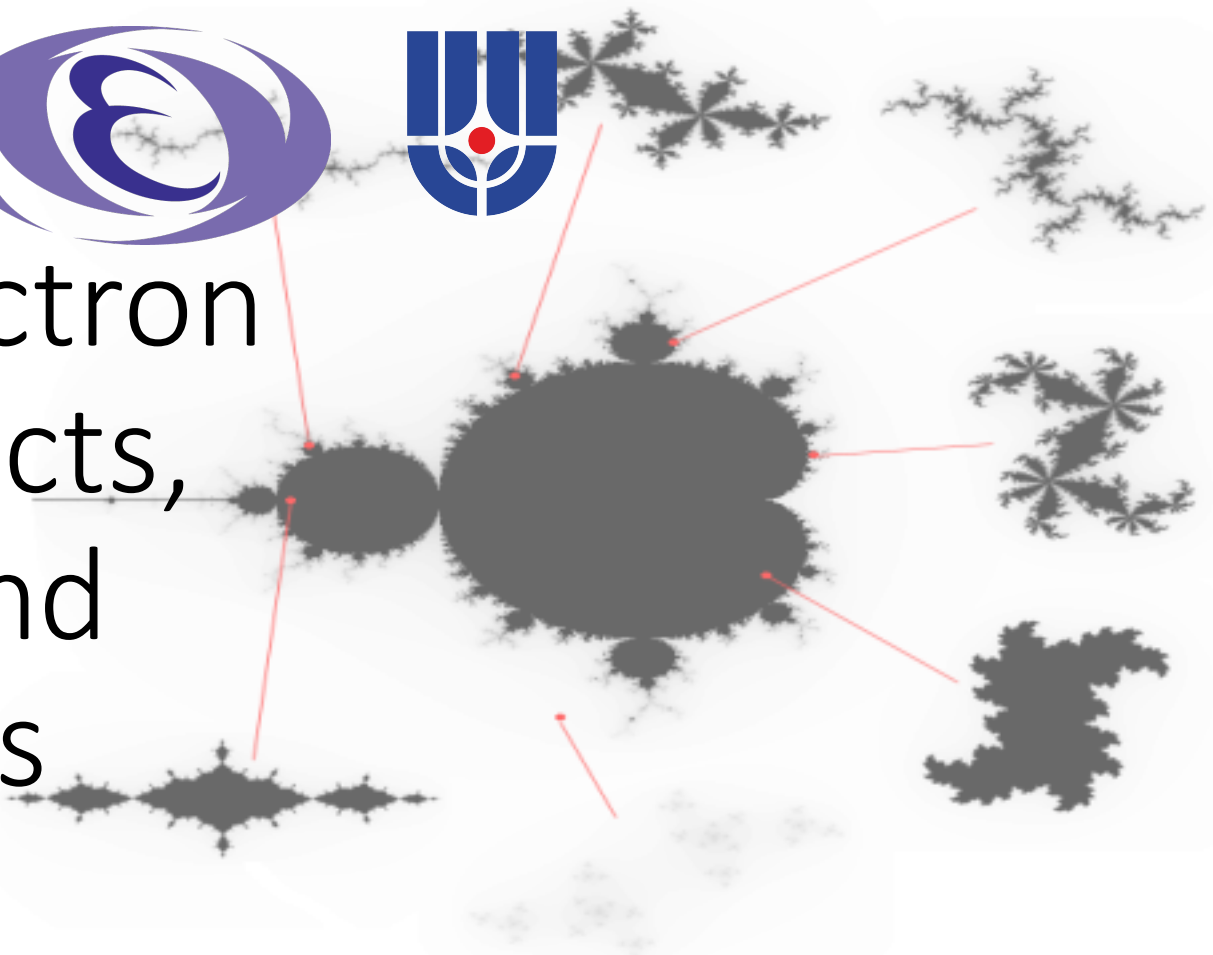


Self-similar electron beam: prospects, demands, and applications



A. Aryshev¹, D.Yu. Sergeeva^{2,3}, M. Shevelev⁴, L.G. Sukhikh⁴, A.A. Tishchenko^{2,3}, N. Terunuma¹ And J. Urakawa¹.

¹ KEK: High Energy Accelerator Research Organization, 1-1 Oho, Tsukuba, Ibaraki 305-0801, Japan .

² National Research Nuclear University (Mephi), Kashirskoe Shosse 31, Moscow, 115409, Russia.

³ National Research Center “Kurchatov Institute”, Akademika Kurchatova Pl. 1, Moscow, 123098, Russia

⁴ Tomsk Polytechnic University, Lenin Avenue 30, Tomsk 634050, Russia

Outline

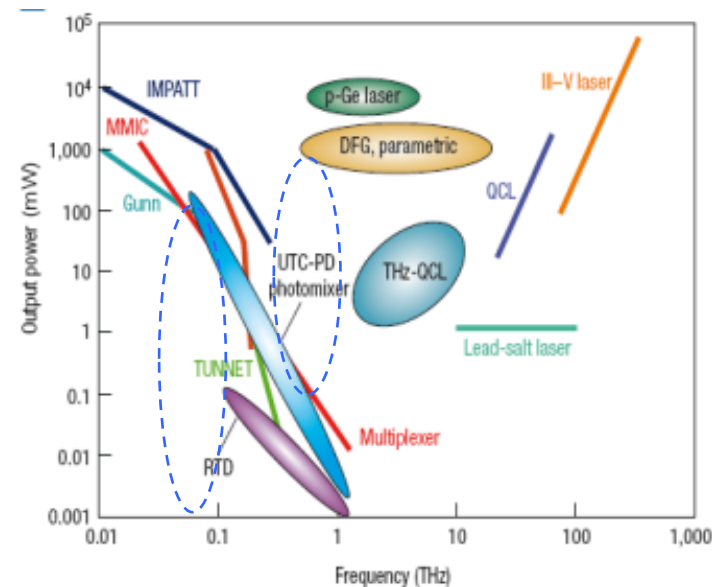
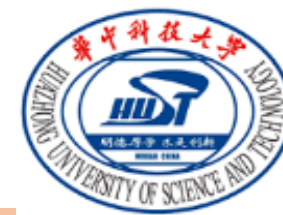
- General motivation
 - Pre-bunched THz FEL and pre-bunched beam effect onto polarization radiations.
- Present experience of longitudinal and transverse e-beam shaping in RF guns.
- A concept of self-similar beams.
- LUCX facility.
- Fractal beam generation .
- Michelson interferometer as a direct time-domain analyzer.
- Conclusion and summary.

Motivation

- Construction of a stable and tunable laser system for RF gun development and THz radiation sources tests based on modern technology.
- Build a broad collaborative network among leading institutions worldwide.
- Develop state-of-the-art tunable coherent THz radiation sources on the basis of a compact (preferably table-top) accelerator.



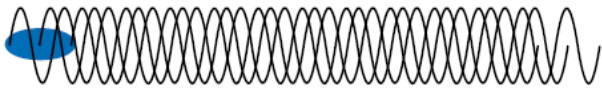
collaboration network



MASAYOSHI TONOUCHI
Institute of Laser Engineering,
Osaka University, Japan

The properties of Coherent Radiation

Incoherent



Coherent

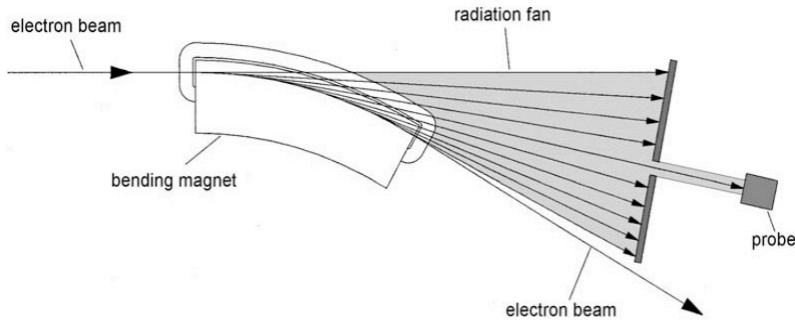


$$\frac{d^2P}{d\Omega d\omega} \approx [N + N^2 \cdot F(\sigma_z, \lambda)] \left| \frac{d^2P}{d\Omega d\omega} \right|_{\text{single } e^-}$$

$$\text{Form-factor: } F(\sigma_z, \lambda) = \left| \int_{-\infty}^{\infty} \frac{1}{\sqrt{2\pi\sigma_z^2}} \cdot \exp\left(-\frac{z^2}{2\sigma_z^2}\right) \cdot \exp\left(i \cdot 2\pi \cdot \frac{z}{\lambda}\right) dz \right|^2 = \exp[-4(\pi\sigma_z/\lambda)^2]$$

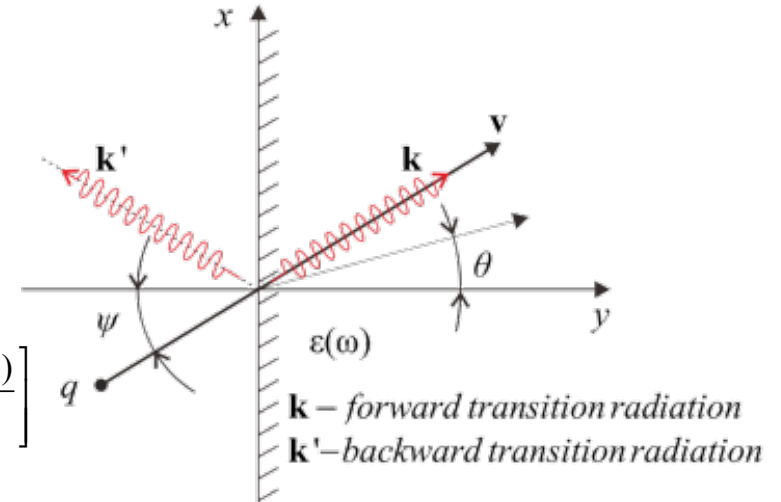
Gaussian distribution of electrons within the bunch

Synchrotron radiation



- ✓ Extreme sensitivity to the radiative bunch length*
- ✓ Form-factor “cut-off” becomes effective when the rms bunch length becomes longer than $\sim \lambda/2$

Transition radiation



$$h(z) = \frac{1}{\sqrt{2\pi\sigma_z^2}} \exp\left[-\frac{z^2}{2\sigma_z^2}\right]$$

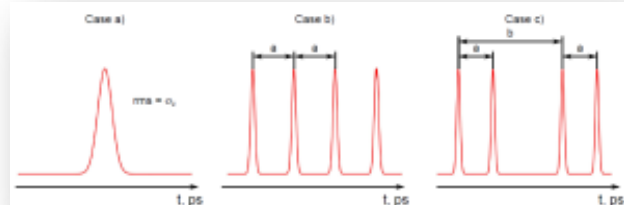
$$f(k) = \exp\left[-\left(\left[k\sigma_\rho \sin\theta\right]^2 + \left[\frac{k\sigma_z}{\beta}\right]^2\right)\right]$$

Coherent form factor dependents on:

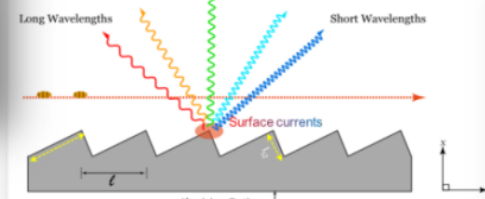
- ✓ angle of observation.
- ✓ transverse size of bunch.
- ✓ longitudinal size of bunch.

Where k – wave number, θ – observation angle, β - the velocity of electron in the units of speed of light

Bunched beam case



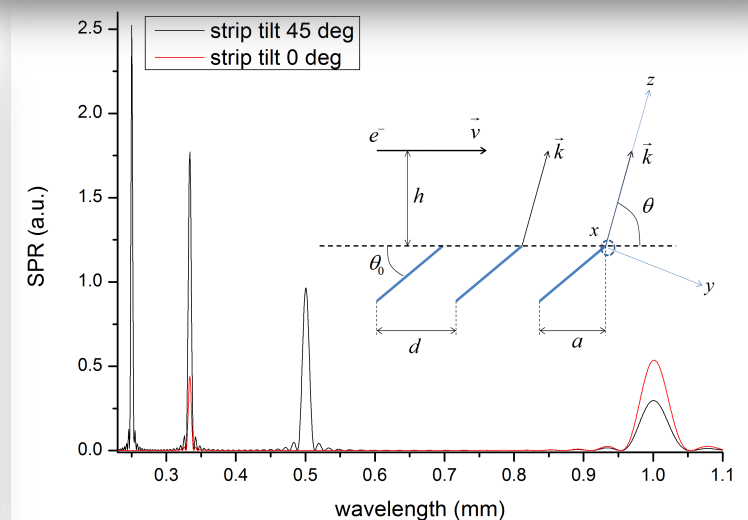
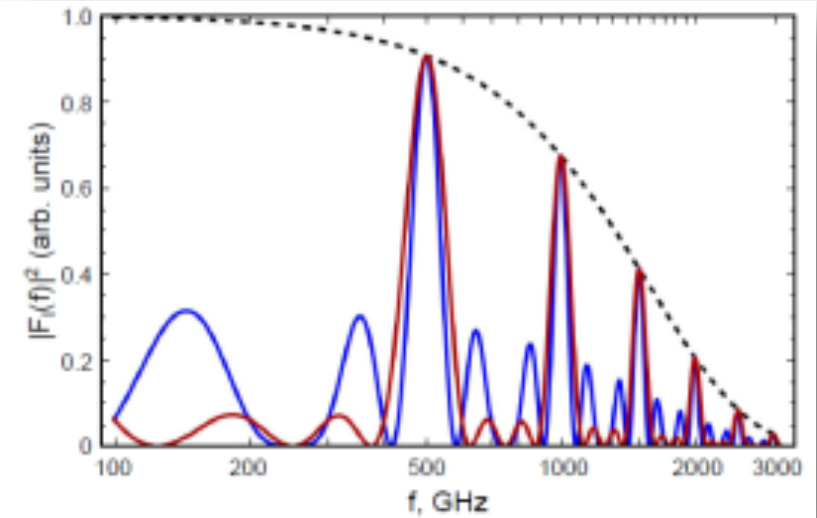
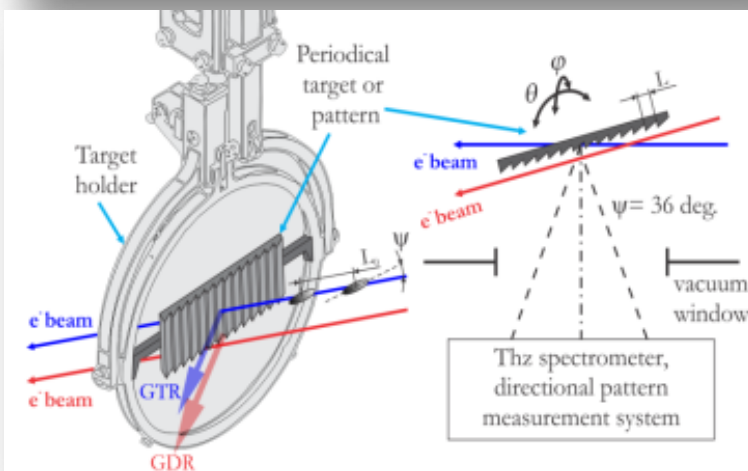
$$\frac{d^2W_{tot}^s}{d\omega d\Omega} = \frac{d^2W_{sing}}{d\omega d\Omega} N_e (1 + (N_e - 1) |f_l(\omega)|^2)$$



$$|F_l^a(f)|^2 = \exp\left(-\frac{4\pi^2 f^2 \sigma_z^2}{\beta^2}\right)$$

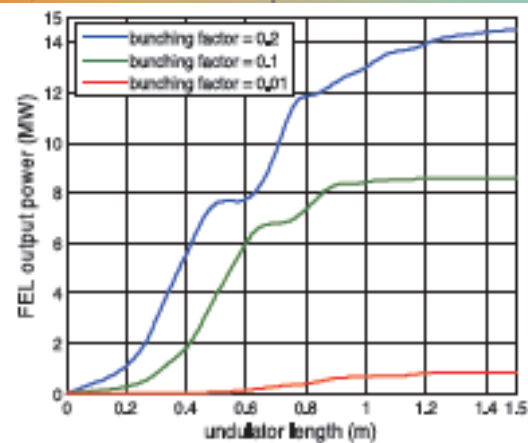
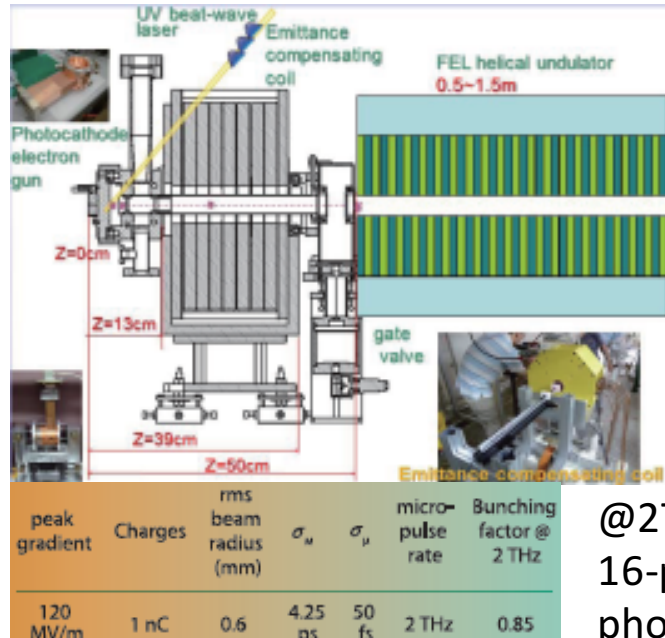
$$|F_l^b(f)|^2 = \frac{1}{N_b^2} \exp\left(-\frac{4\pi^2 f^2 \sigma_z^2}{\beta^2}\right) \frac{\sin^2\left(N_b \frac{\pi f}{\nu_m}\right)}{\sin^2\left(\frac{\pi f}{\nu_m}\right)}$$

$$|F_l^c(f)|^2 = \frac{1}{4} \exp\left(-\frac{4\pi^2 f^2 \sigma_z^2}{\beta^2}\right) \left(1 + \cos\left(\frac{2\pi a f}{\beta}\right)\right) \left(1 + \cos\left(\frac{2\pi b f}{\beta}\right)\right)$$

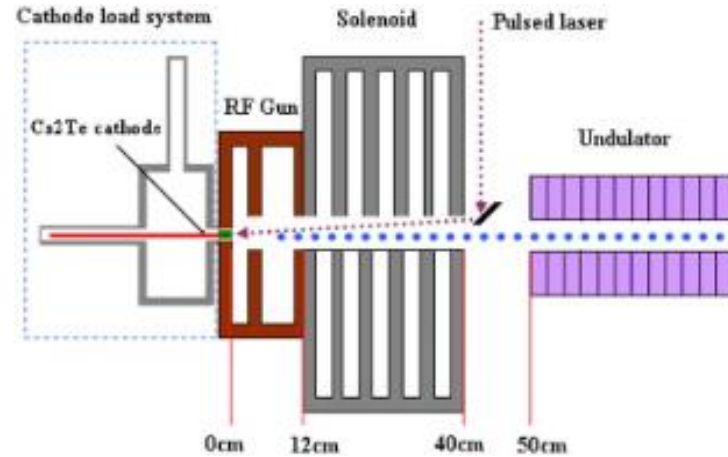


Compact pre-bunched generation schemes

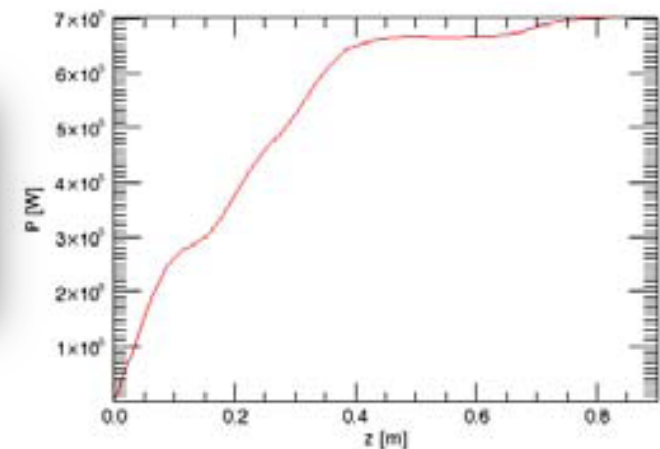
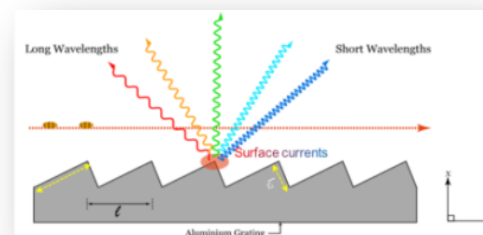
Prof. Y.-C. Huang, National Tsinghua University,
Hsinchu, Taiwan



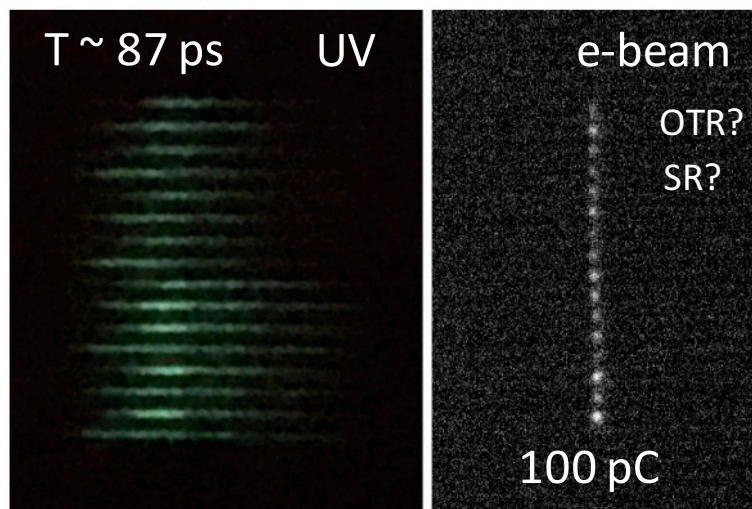
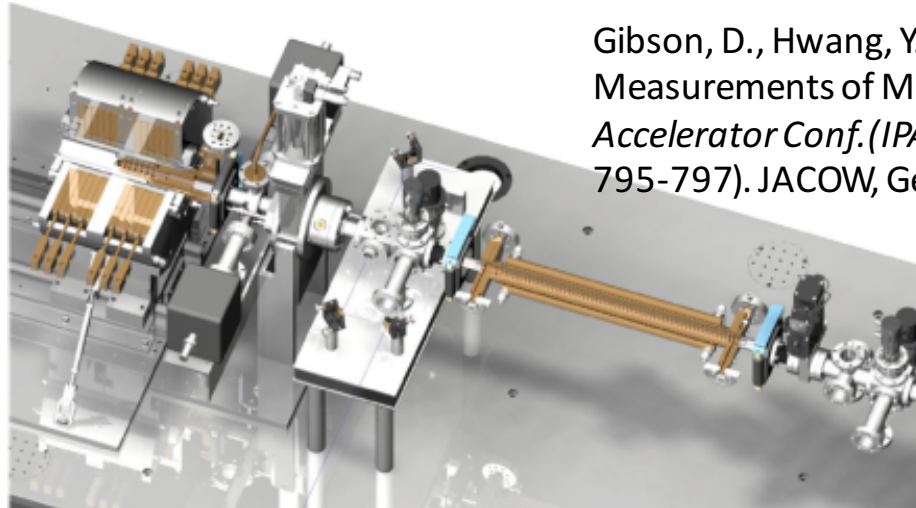
Shengguang Liu, Yen-Chieh Huang, NIM A 637 (2011)
S172–S176



@2THz (150 um), time spacing between laser pulses is 500fs.
16-pulse train of 50fs. Pulse train charge more than 200pC,
photocathode Q.E. 1%. Peak power at megawatt(MW) level, 0.1 mJ



LLNL: linac-driven, laser-based Compton scattering gamma-ray source



Gibson, D., Hwang, Y. and Marsh, R., 2017, May. Initial Performance Measurements of Multi-GHz Electron Bunch Trains. In *8th Int. Particle Accelerator Conf. (IPAC'17), Copenhagen, Denmark, 14â19 May, 2017* (pp. 795-797). JACOW, Geneva, Switzerland.

R.A. Marsh et al., "Modeling and Design of an X-Band RF Photoinjector", Phys. Rev. ST Accel. Beams, vol. 15, p. 102001, 2012.

Frequency	11.424 GHz
Unloaded quality factor	7055
First cell length	0.59 cell
Coupler type	Dual feed racetrack
Iris shape	Elliptical, 1.8 major/minor
Mode separation	25 MHz
Cathode material	Oxygen-free high conductivity
Cathode peak field	200 MV/m
Final kinetic energy	7 MeV

RF Gun laser

Wavelength	263.25 nm
Energy	50 μ J
Transverse σ	0.55 mm
Transverse hard edge	0.46 mm
Temporal rise/fall	250 fs
Temporal FWHM	2 ps

Interference-related methods

Neumann, J. G., Fiorito, R. B., O'Shea, P. G., Loos, H., Sheehy, B., Shen, Y., & Wu, Z. (2009). Terahertz laser modulation of electron beams. *Journal of Applied Physics*, 105(5), 053304.

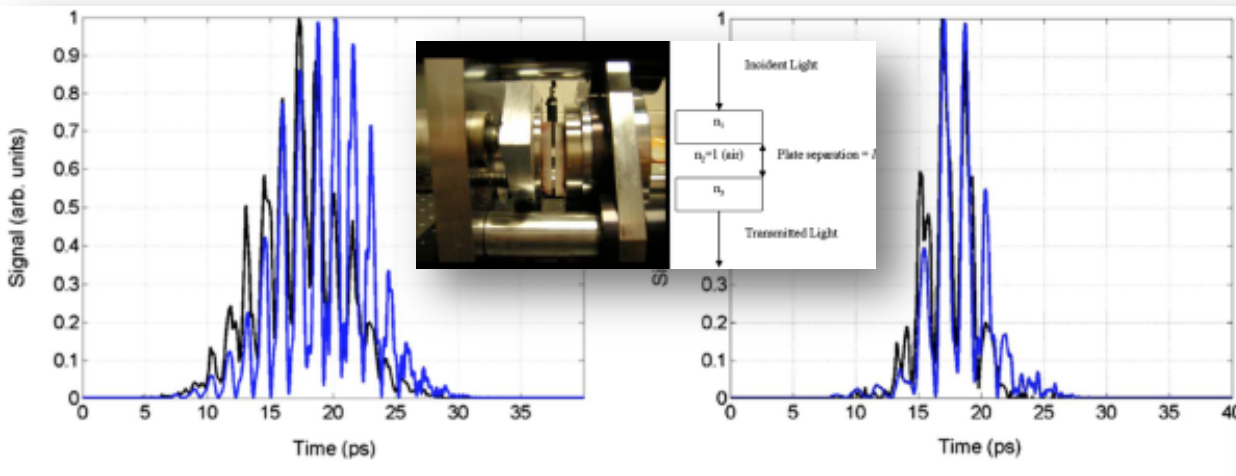


FIG. 7. (Color online) Cross-correlation measurement of modulated laser intensity (blue) compared with theory (black) for a cavity spacing of $260 \mu\text{m}$ (left) and $207 \mu\text{m}$ (right).

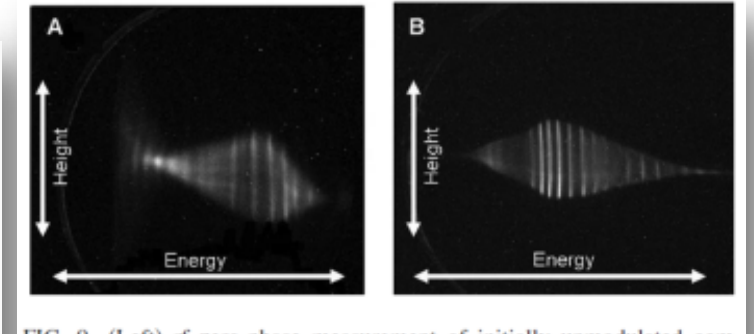
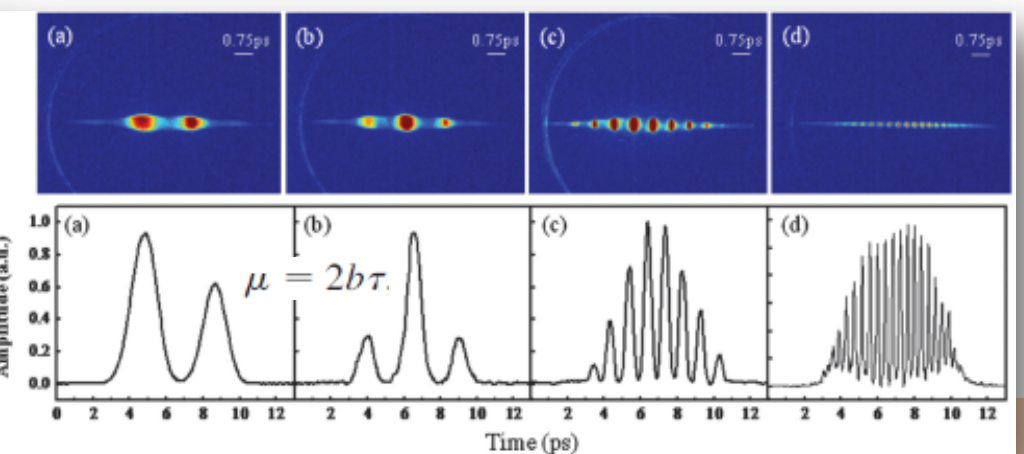
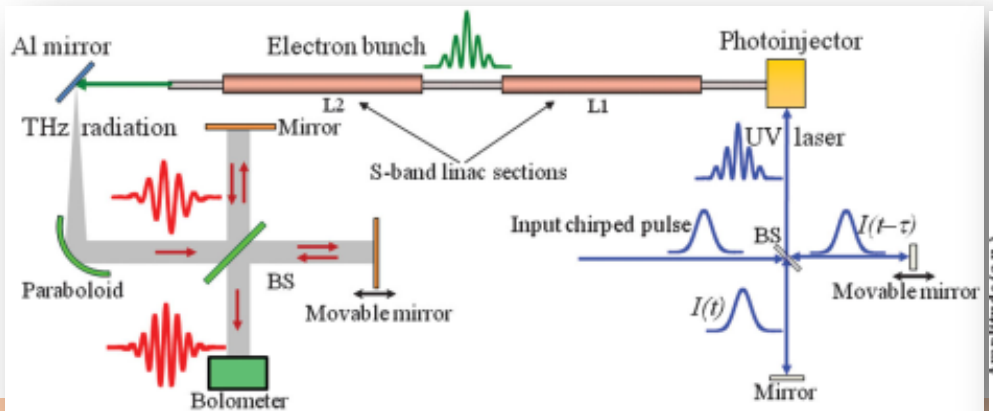


FIG. 9. (Left) rf zero-phase measurement of initially unmodulated compressed electron beam; (right) rf zero-phase measurement of deeply modulated uncompressed electron beam.

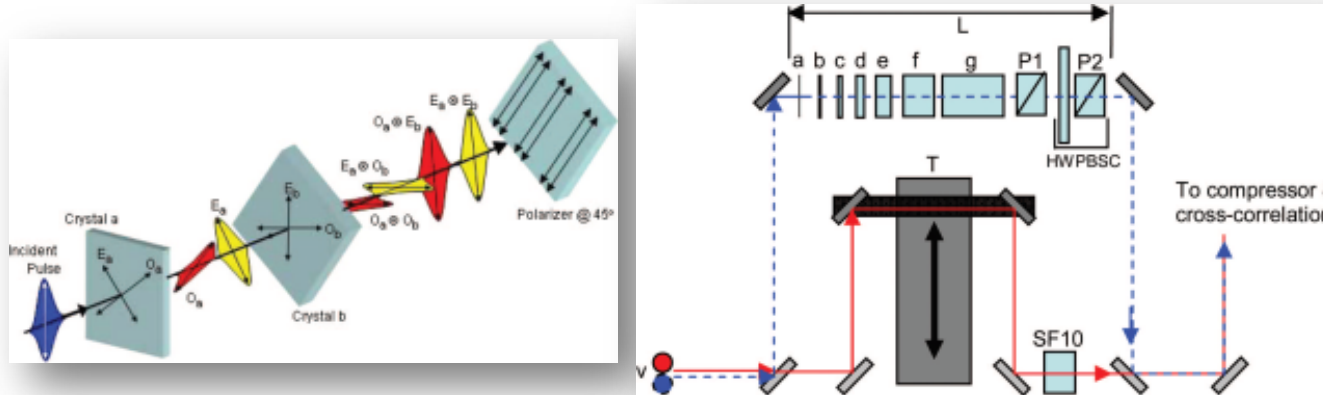
$$I(t, \tau) = |E(t) + E(t + \tau)|^2 = I(t) + I(t + \tau) + 2\sqrt{I(t)I(t + \tau)} \cos(\omega_0\tau + b\tau^2 + 2b\tau)$$

Shen, Y., Yang, X., Carr, G. L., Hidaka, Y., Murphy, J. B., & Wang, X. (2011). Tunable few-cycle and multicycle coherent terahertz radiation from relativistic electrons. *Physical review letters*, 107(20), 204801.



Birefringent crystal array

Dromey, B., Zepf, M., Landreman, M., O'keeffe, K., Robinson, T., & Hooker, S. M. (2007). Generation of a train of ultrashort pulses from a compact birefringent crystal array. *Applied optics*, 46(22), 5142-5146.



$$\Delta t = x \left(\frac{1}{V_o} - \frac{1}{V_e} \right)$$

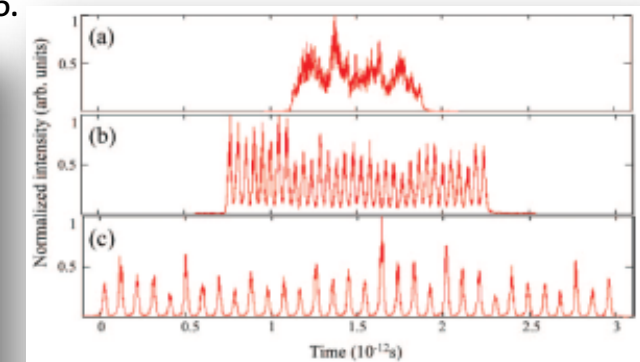
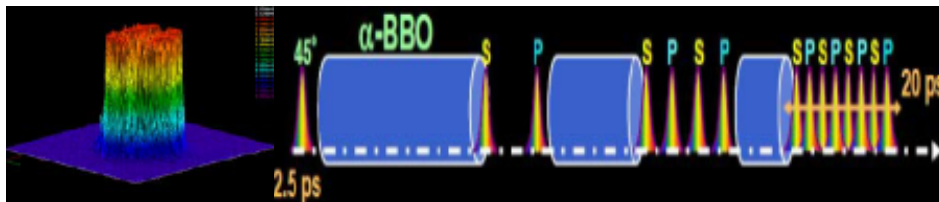


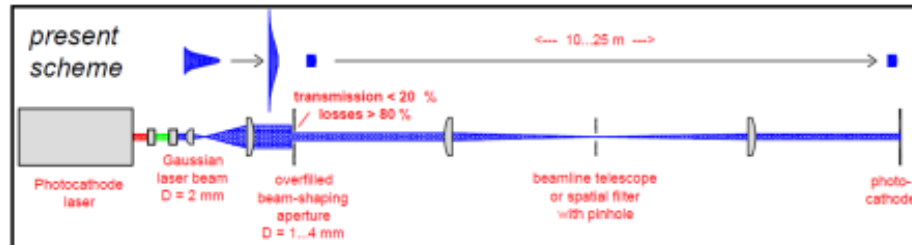
Fig. 5. (Color online) Cross correlation traces of the pulse train with the probe beam pulse performed on the Oxford 125 fs pulse duration Ti:sapphire laser. The following crystal configurations were used: (a) first five crystals in, sixth and seventh crystal out, 32 pulses with minimum separation; (b) first and last crystal out, crystals two through six in, 32 pulses with two times minimum separation; (c) first and second crystal out, crystals three through seven in, 32 pulses with four times minimum separation.

Giorgianni, F., Anania, M.P., Bellaveglia, M., Biagioni, A., Chiadroni, E., Cianchi, A., Daniele, M., Del Franco, M., Di Giovenale, D., Di Pirro, G. and Ferrario, M., 2016. Tailoring of highly intense THz radiation through high brightness electron beams longitudinal manipulation. *Applied Sciences*, 6(2), p.56.

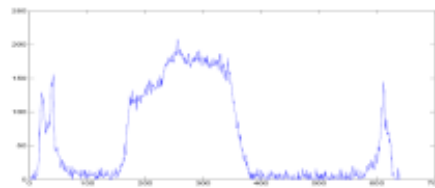
Yan, L., Du, Q., Du, Y., Hua, J., Huang, W. and Tang, C., 2011. UV pulse shaping for the photocathode RF gun. *Nuclear Instruments and Methods in Physics Research Section A: Accelerators, Spectrometers, Detectors and Associated Equipment*, 637(1), pp.S127-S129.



Gaussian to flat top clipping: PITZ and ATF/DESY



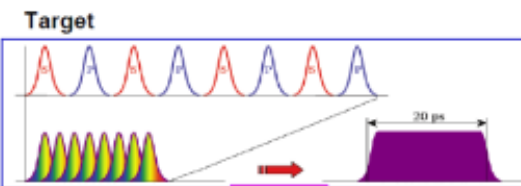
- Imaging the overfilled iris on laser table
- Problem: larger pointing jitter than iris in front of vacuum
- Jitter about 0.5 of diameter min/max



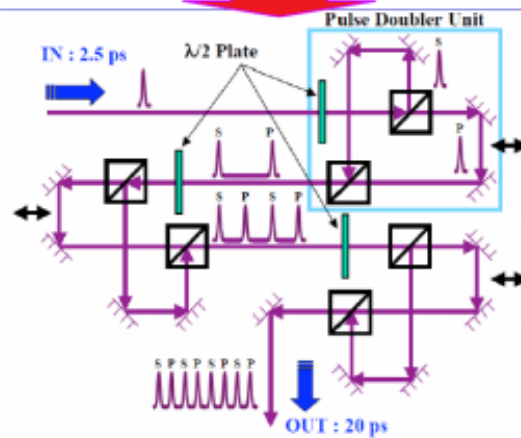
Ingo Will, Max-Born Institute
S. Schreiber, DEZY

PITZ mini pulse shaping workshop, 2007

Implementation at Spring8

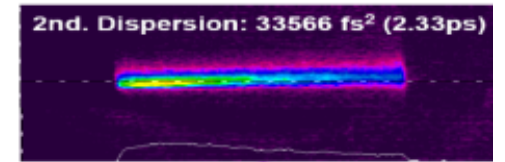
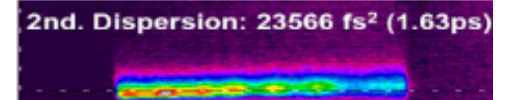


Scheme

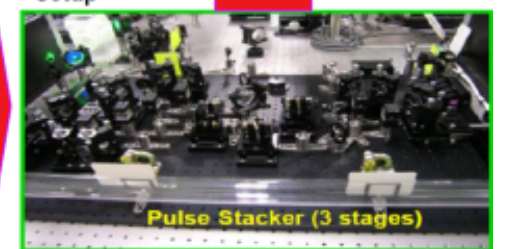


Beam clipping

Results

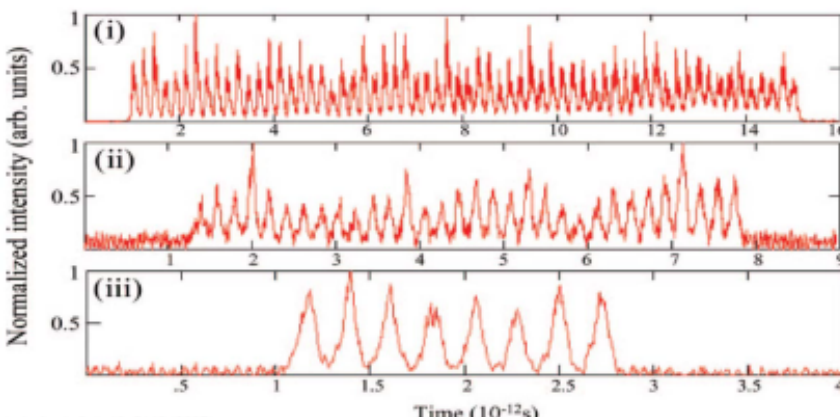
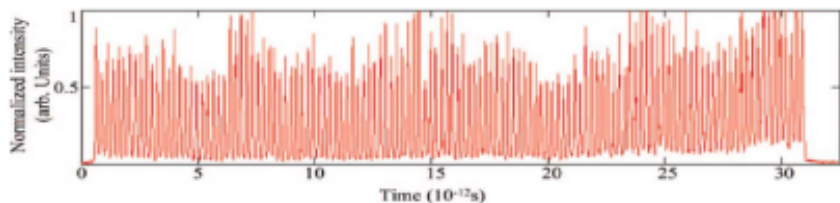


Setup

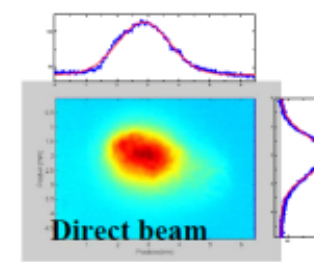


Tomizawa, Quantum Electronics 37, 697 (2007)

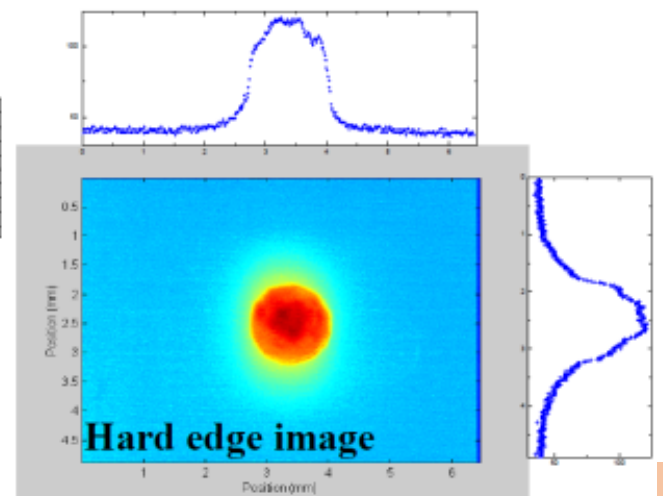
Results, for pulse trains at 800 nm



- Self-explaining but obvious far from perfect and low efficiency

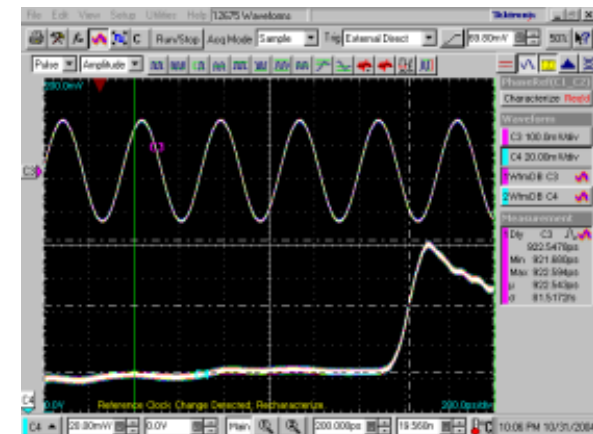
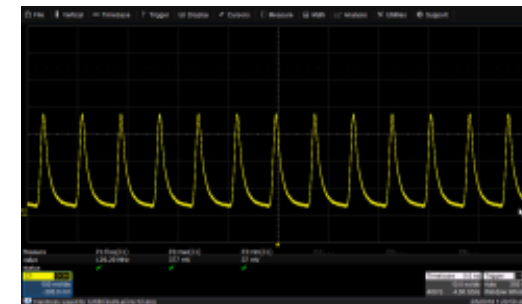
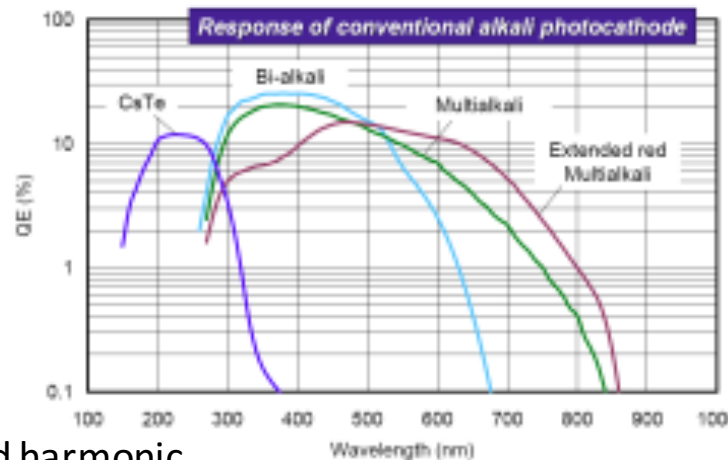


- BNL TTF
- APS PC gun
- LCLS



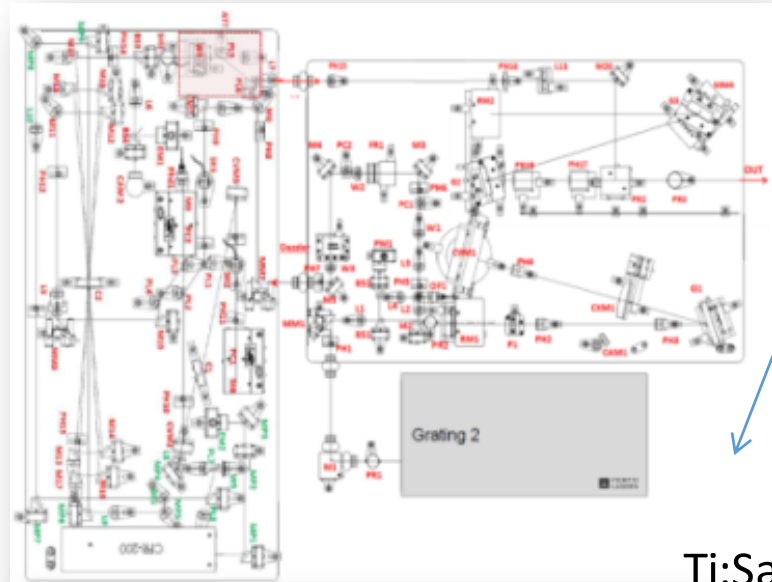
Typical laser pulse parameter requirements for RF gun photocathode

- Pulse energy, **> 10uJ** for Cs₂Te
- Pulse duration, **~ 100fs – 10ps**
 - Space-charge limited
- Wavelength, **~ 250nm** for Cs₂Te
 - Hence, High Harmonic Generation is needed
 - Conversion efficiency depends on pulse duration and harmonic
- Pulse repetition rate
 - Hz (machine), MHz (multi-bunch), GHz-THz (micro-bunch)
- Timing stability, **< 1ps** (~1 deg. RF phase (2.8GHz))
 - Stabilized and synchronized oscillator
 - Stabilized Laser Transport Line
- Pointing stability, smaller than rms spot size, typ **< 100um**.
 - Stabilized Laser Transport Line
 - Additional spatial filters
- Spatial and temporal pulse shaping
 - Pulse stacking
 - Micro-lens arrays
 - π -shapers



RF Gun laser system technologies

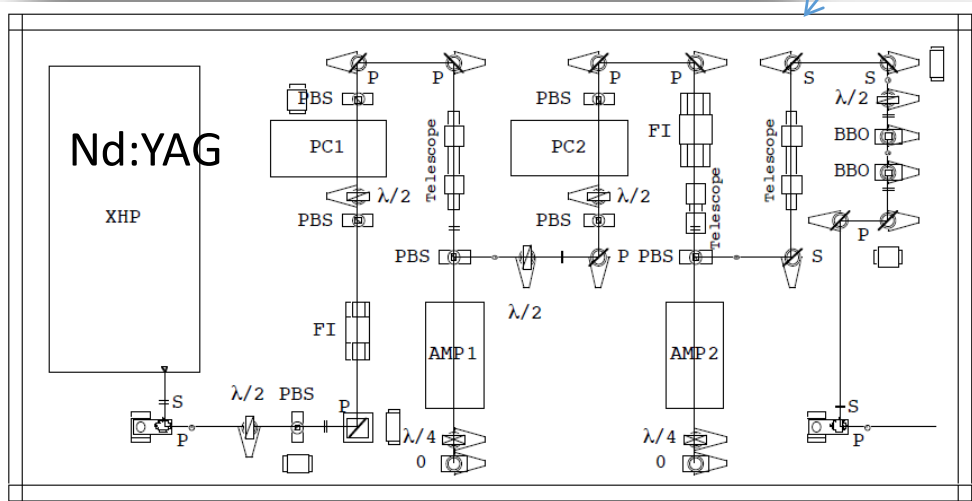
- Solid-state-based technology



Hz rep.rate
fs pulse
High Energy
Complexity

Hz rep.rate
ps pulse
High Energy
Simplisity

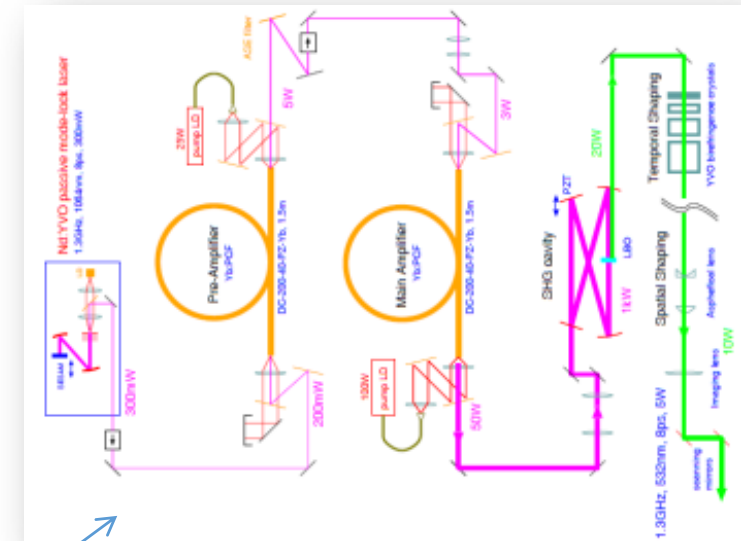
Ti:Sa



MHz rep.rate
~100 fs pulse
Low Energy
Simplisity

- Fiber-based technology

Yb-dopped fiber for example



courtesy Y. Honda

A. Chong, W.H. Renninger, F. W. Wise, Opt. Lett. 33 (2008) 2638:

Numerical simulations of Yb-doped fiber lasers indicate that ~30 fs pulses are possible for a realistic design with off-the-shelf components. Experiments are constrained by the available pump power, but ~75 fs pulses are obtained. (just for oscillator !!!)

Er-doped fiber laser is also promising candidate

What's so Special About ps-fs Lasers?

Short optical pulse.

- Most of energy dissipation and transfer processes occur on the time scale larger than 100 fs.
- Femtosecond laser pulses enable one to generate electron bunches with similar durations (strongly related to generation of THz radiation).
- Specific laser system design approaches.
- Specific gain materials due to optical BW and efficiency with fs pulses.
- Specific pulse diagnostics.

High peak power of the light

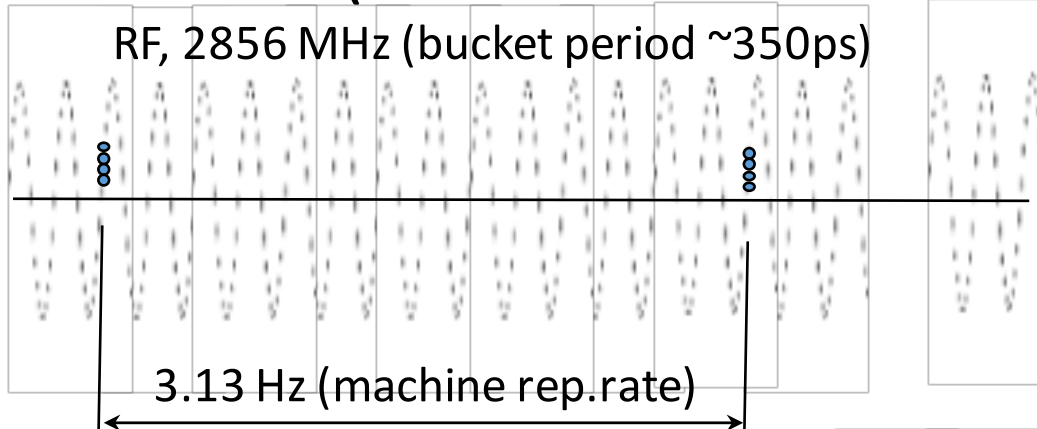
- $I \sim J/T_{pulse}$, I – Power, J – pulse energy.
 - 1 mJ pulse with 10 ns duration - **0.1 MW**.
 - 1 mJ pulse with 100 fs duration - **10 GW**.
- Non-linear response of the optical components(e.g., multi-photon absorption, optical harmonics generation, materials ablation, etc.)

Large bandwidth

- Broadband optical components (mirrors, etc)
- Achromatic lens, waveplates, etc.
- Higher demands for laser safety.

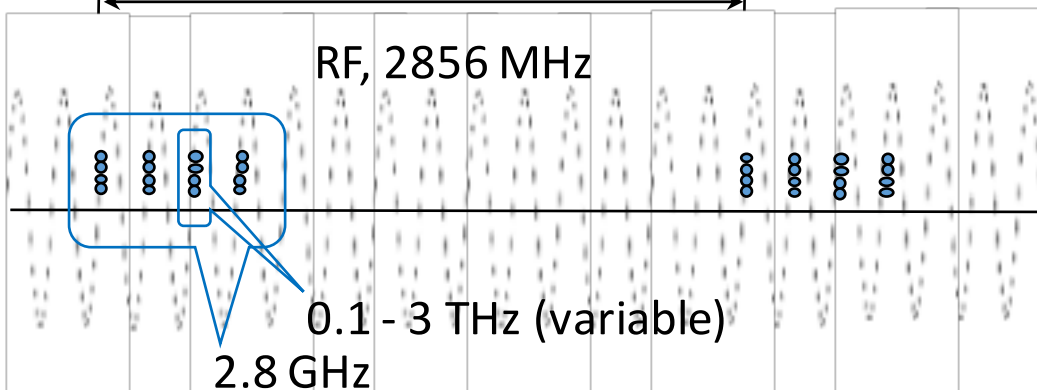
W. Kaiser, ed., “*Ultrashort Laser Pulses: Generation and Applications*”, Springer-Verlag, Berlin, **1993**

Multi-micro-bunch bunches (self-similar or “Fractal beam”.)



4 micro-bunches
1 multi-bunch (1 RF bucket)

- Number of filled RF buckets depends only on FH laser energy budget
- Non-sequential RF bucket filling is possible



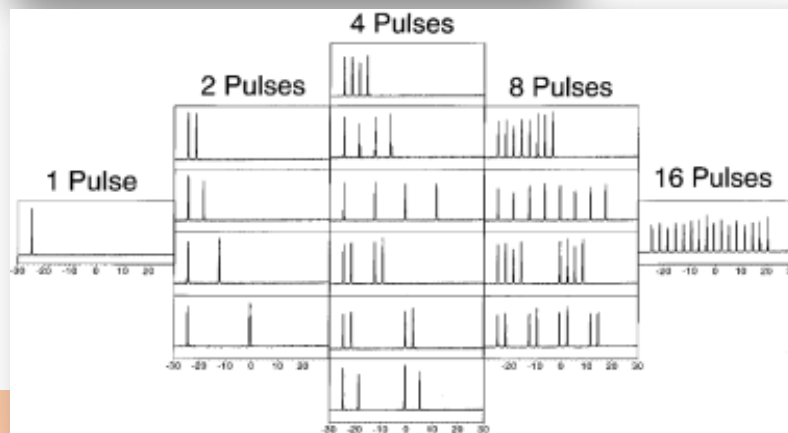
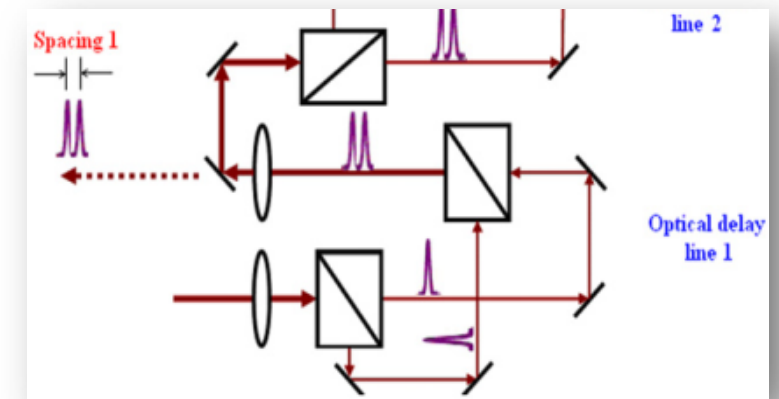
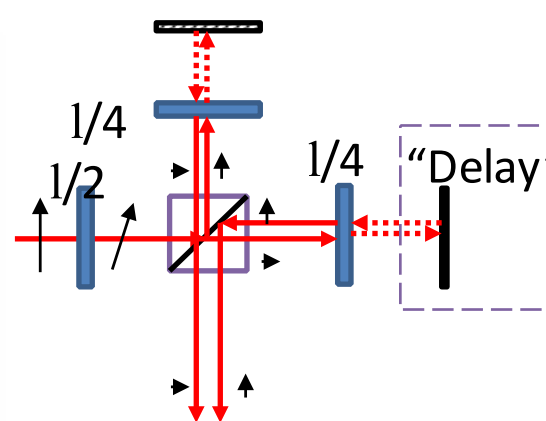
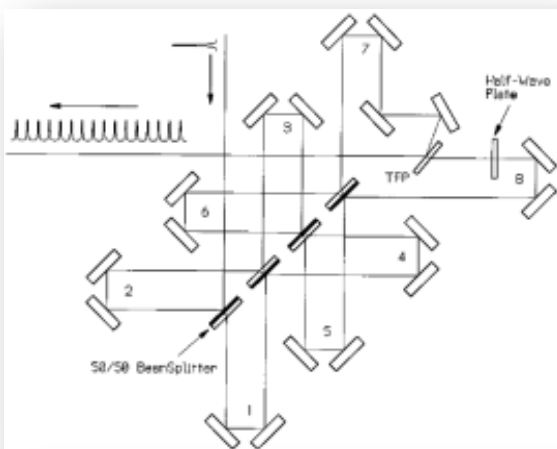
4 micro-bunches
4 multi-bunch (4 RF buckets)

- DAQ sees this micro-train as a single event (no trigger modification is required)
- Micro-bunch spacing changing simultaneously in all buckets

- One of the typical S-band accelerator parameters:
 - Multi-bunch rep.rate (from the RF gun laser oscillator) ~ 357MHz (every 9th RF bucket)
 - RF pulse width ~ 4 us => max 1400 bunches (roughly) – filling time etc. ~ 1250 bunches
- Applying 8-times pulse split -> 10000 bunches/4 us !!!
- Effects on: X-ray Compton, Fiber laser oscillators implementation, total radiated power.

Pulse splitter

- C.W. Siders et al., "Efficient High-Energy Pulse-Train Generation using a 2n-Pulse Michelson Interferometer", Appl. Opt., vol. 37, p. 5302, 1998.
- Liu, S. and Huang, Y.C., 2011. Generation of pre-bunched electron beams in photocathode RF gun for THz-FEL superradiation. *NIMA*, 637(1), pp.S172-S176.



- These approaches give alternative polarizations within the train.
- What is leading to at least 50% losses on downstream polarization-sensitive laser components (Amplifiers, Compressors, HHG, etc.)

“Buncher”, second (current) prototype

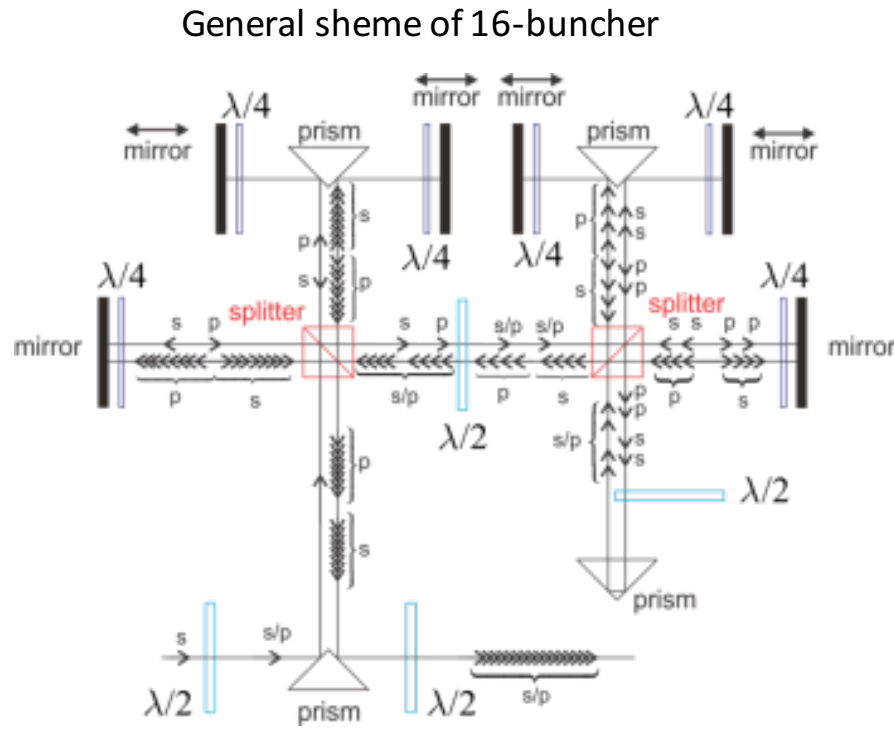
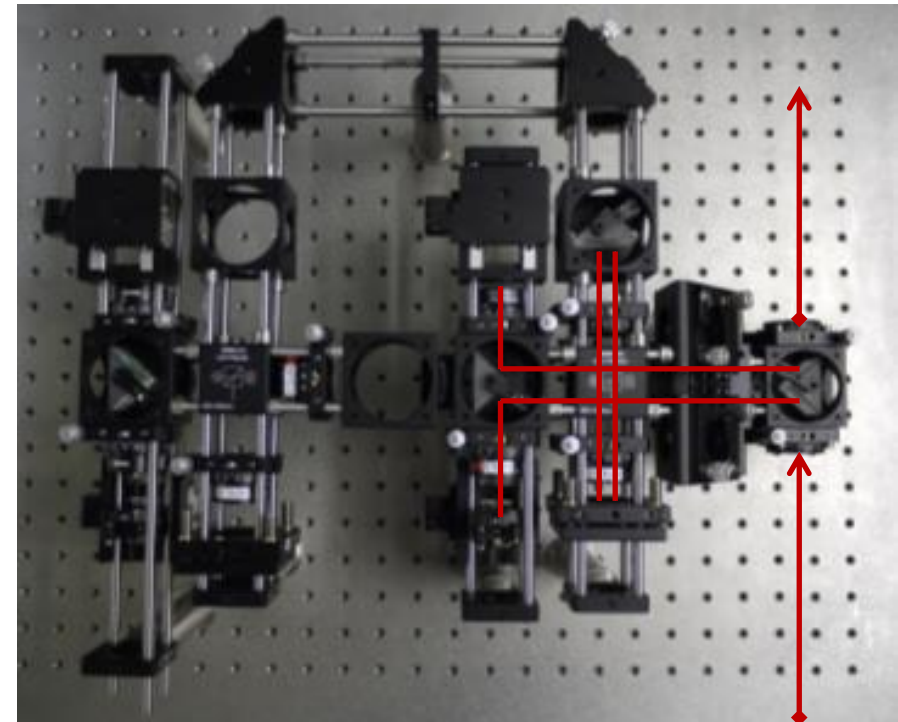


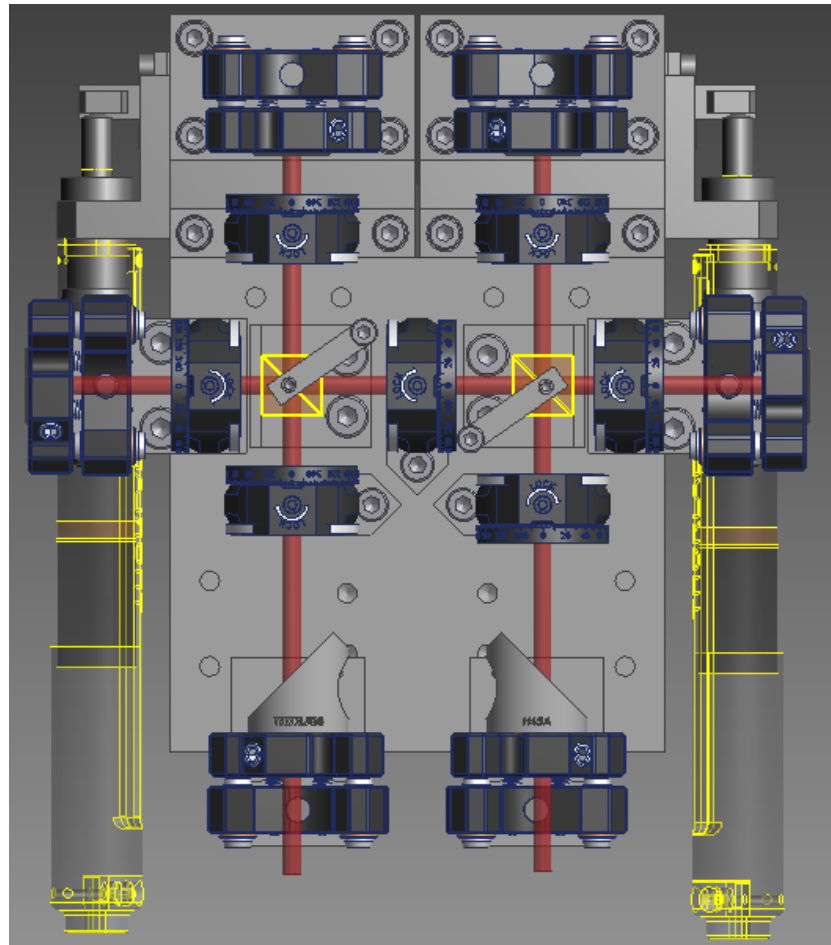
Photo of pre-assembled buncher



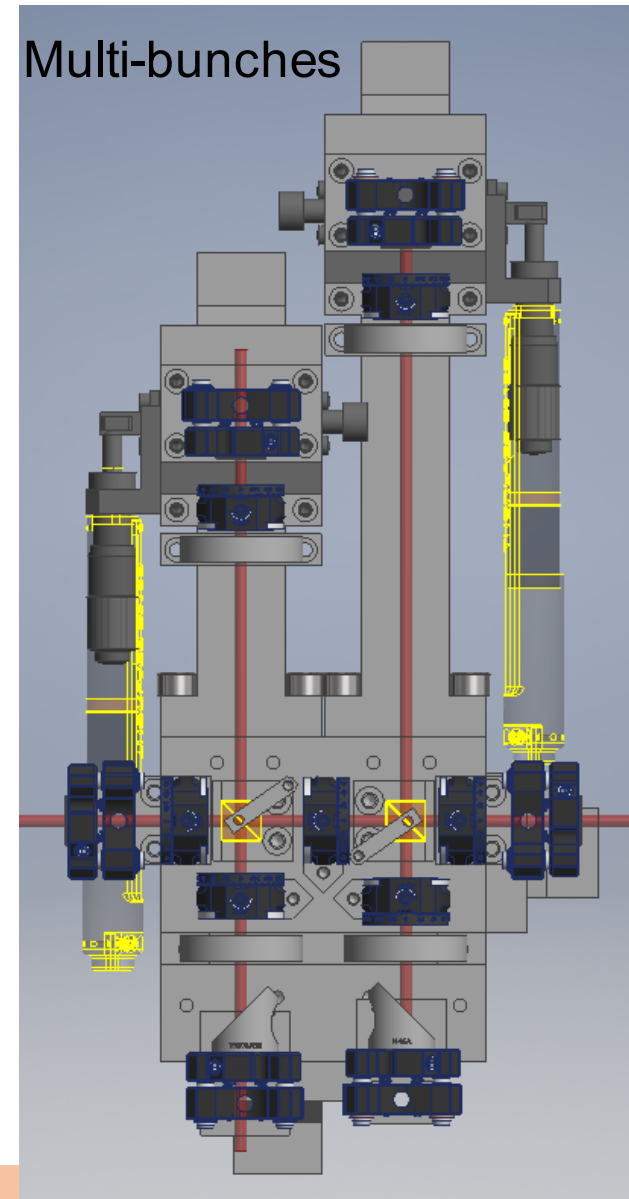
- All bits were delivered in September 2014.
- Assembled and tested (laser side only) in Nov.-Dec. 2014
- Tested (e-beam generation) in Jan. – Feb. 2015

Laser pulse splitter (buncher)

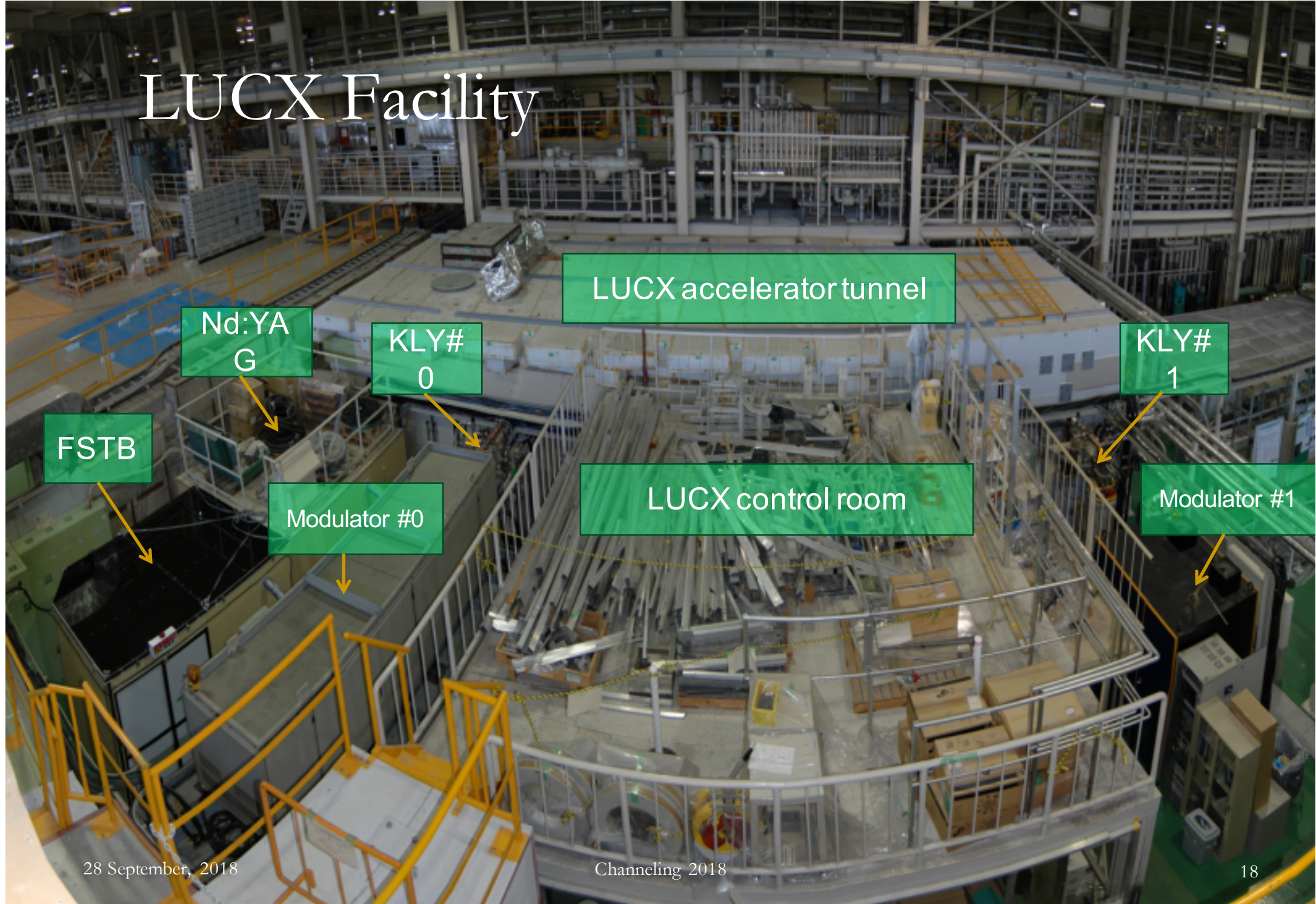
Micro-bunches



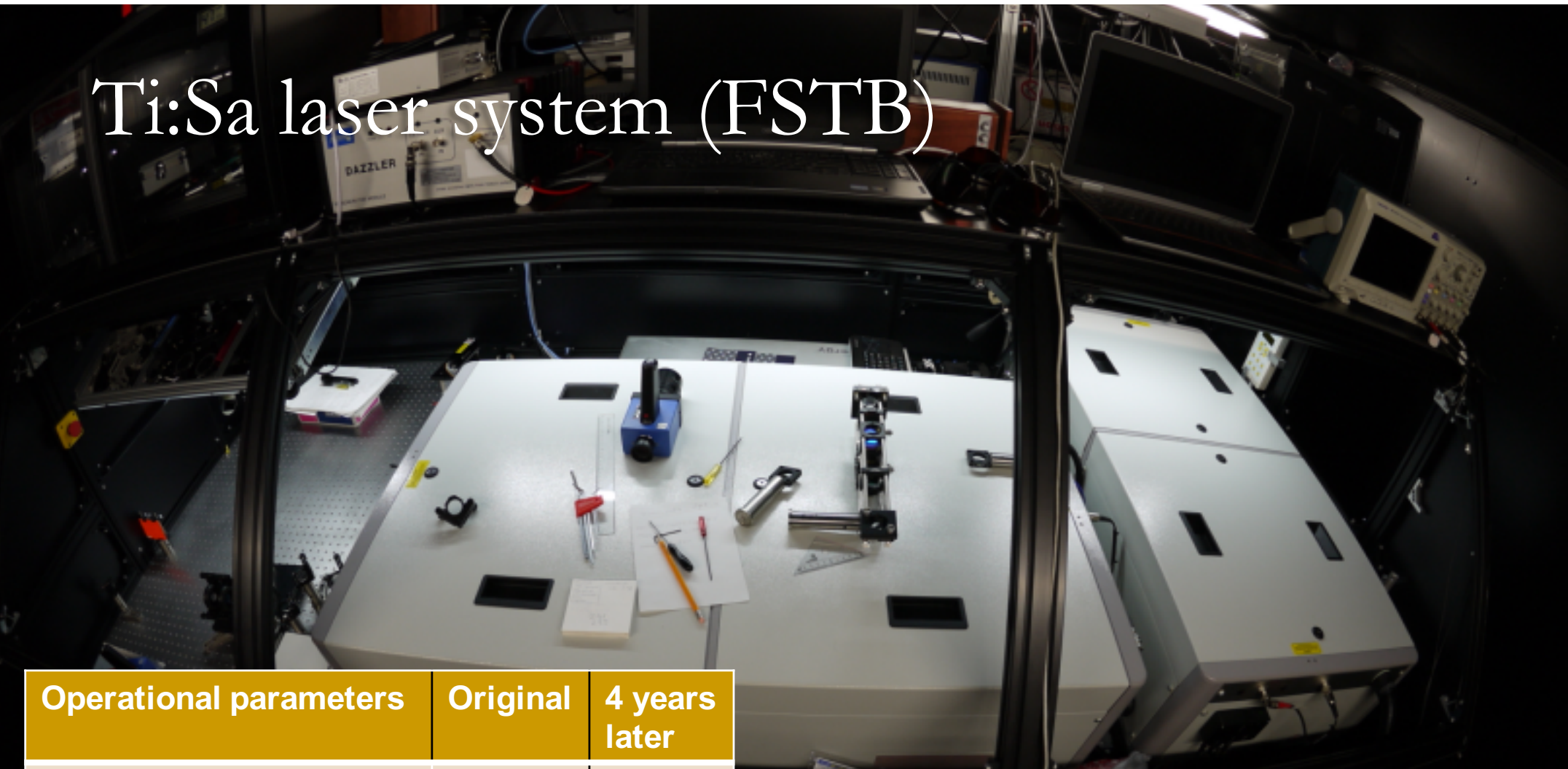
Multi-bunches



LUCX Facility



Ti:Sa laser system (FSTB)

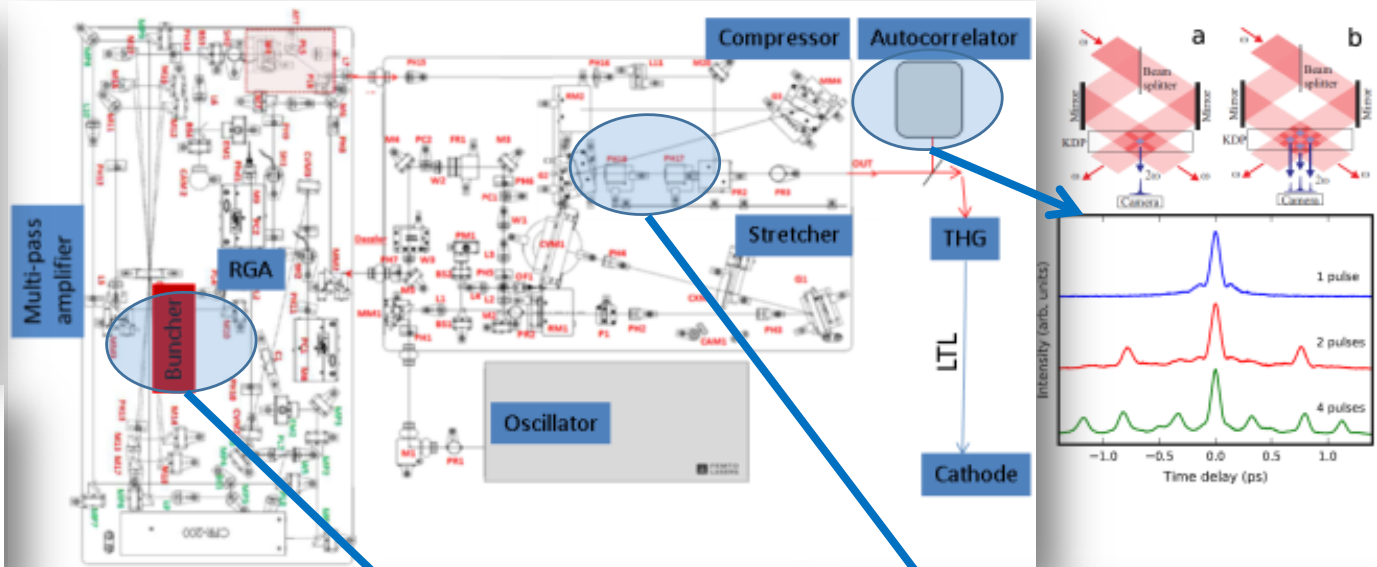
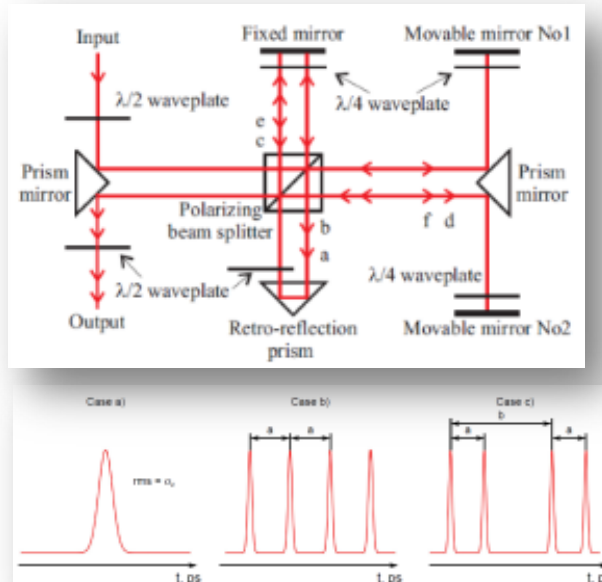


Operational parameters	Original	4 years later
Repetition rate, max	10Hz	3.13Hz
Central wavelength	795nm	795nm
Pulse energy before compression	22mJ	5mJ
Pulse energy after compression	14mJ	3mJ
Pulse duration w/w/o correction	30/37.7fs	50fs
Energy stability 22mJ@800nm	1.6%	3%

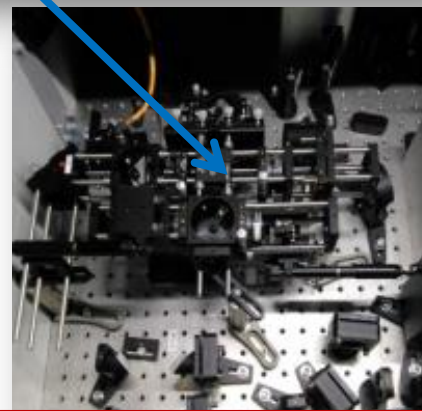
- Entire infrastructure was built
- Control soft 80% re-written
- Additional pulse diagnostics introduced
- THG simulated, ordered, built
- 2 buncher systems were implemented

Multi-micro-bunch, implementation

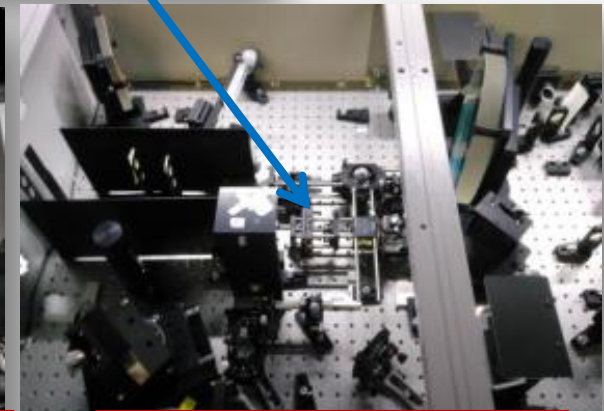
Present condition: 4x4 pulses, ~50 fs each, converted to 266nm, 10uJ



- **Total splitting efficiency ~20%**
- New design with total 10-20% losses is possible.
- Beam expander was removed.
- Multi-pass Amp, Compressor, THG, LTL re-tuned.
- **Micro-bunch**
 - Separation: +/- 5 ps
 - Stability: < 20 fs (lower than meas. resolution)
- **Multi-bunch**
 - Separation: 350ps +/- 30 ps

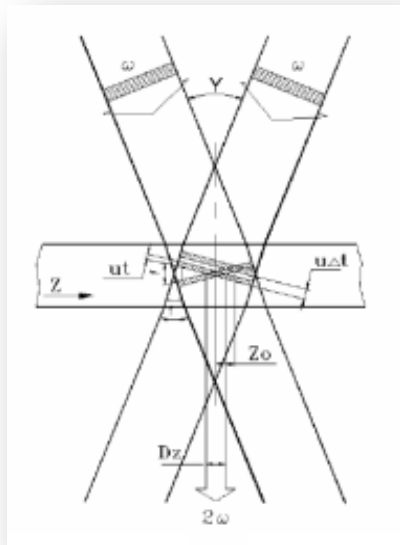


Motorized delay control

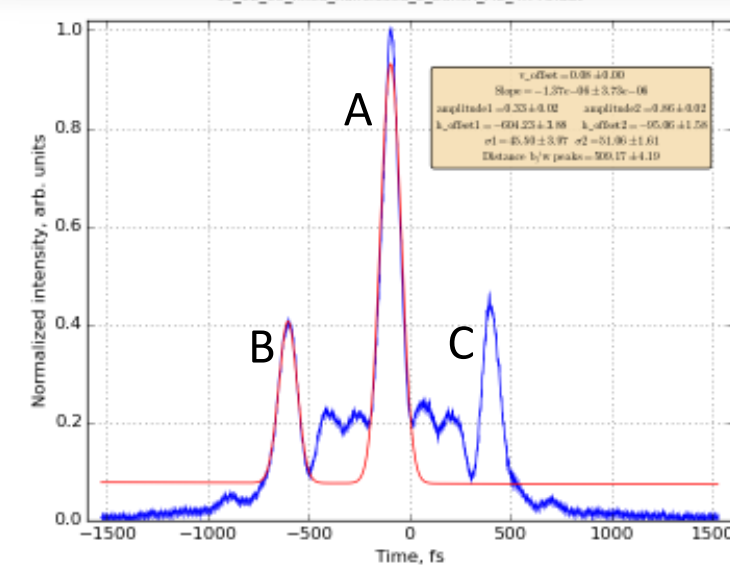
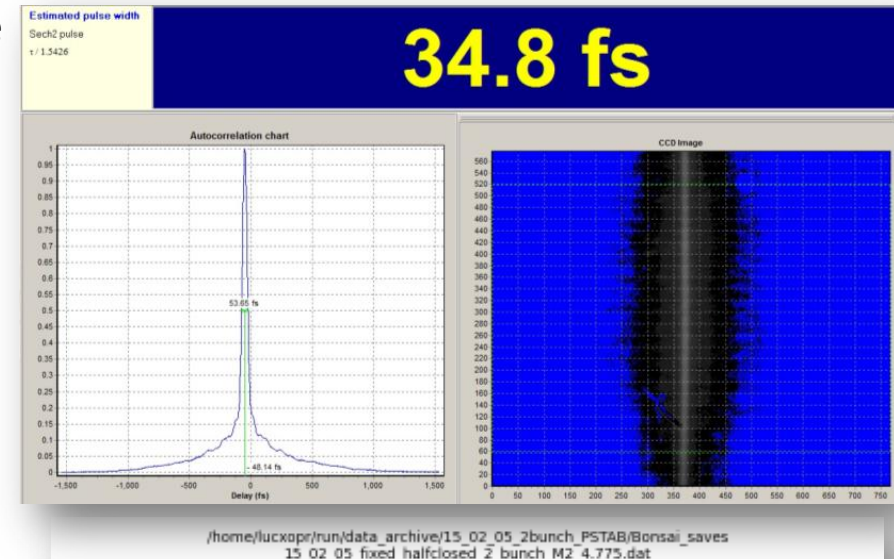
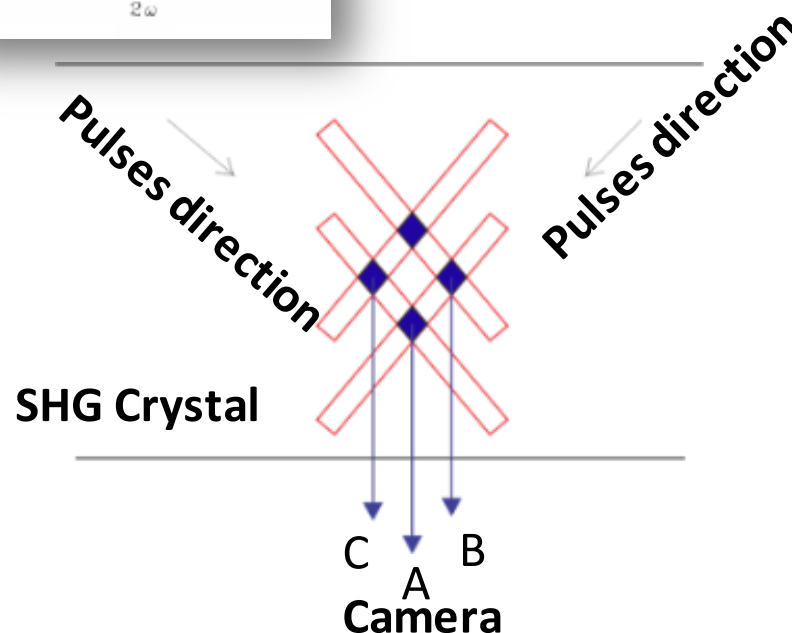


Manual delay control

FSTB: fs Single Shot cross-correlator



The method based on the registration of cross distribution of Second Harmonic (SH) energy produced in nonlinear crystal under non-collinear interaction of two beams with determined aperture.

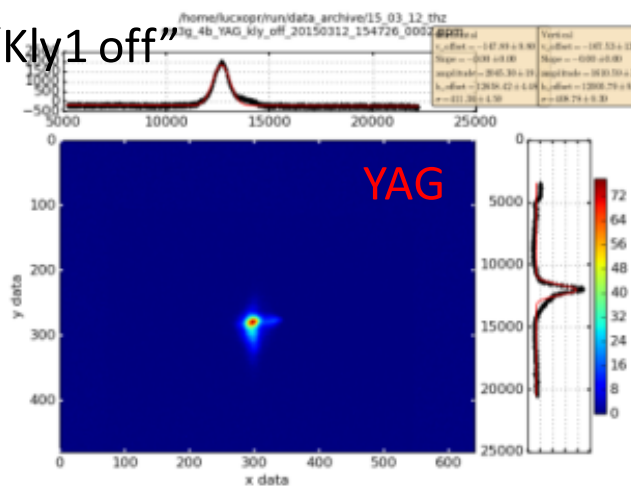


4-micro bunch generation

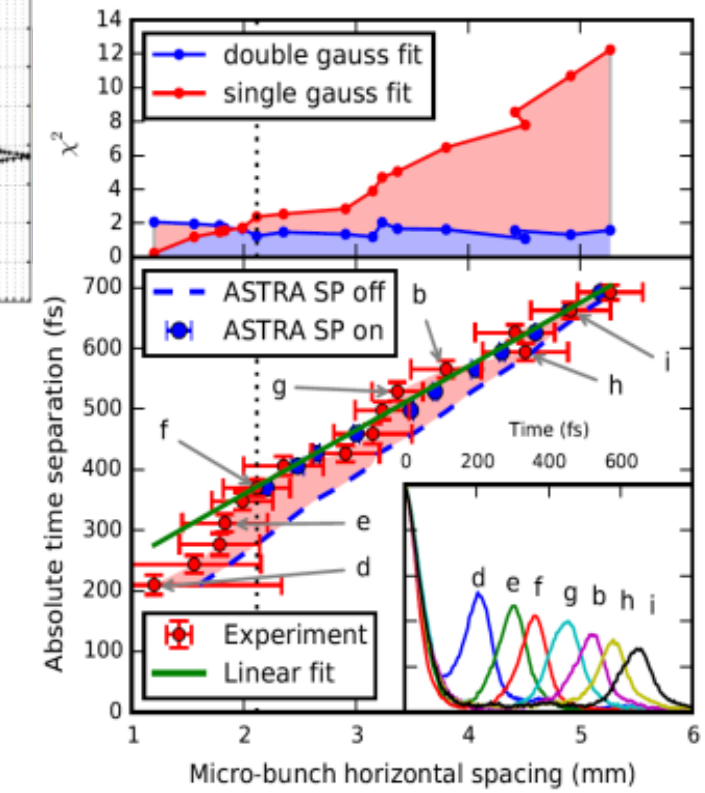
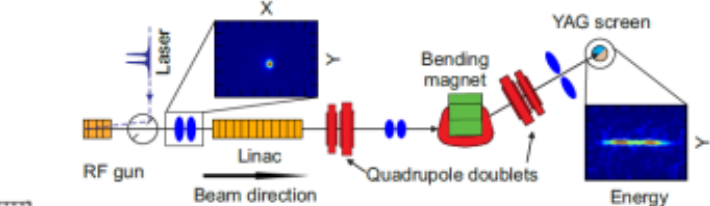
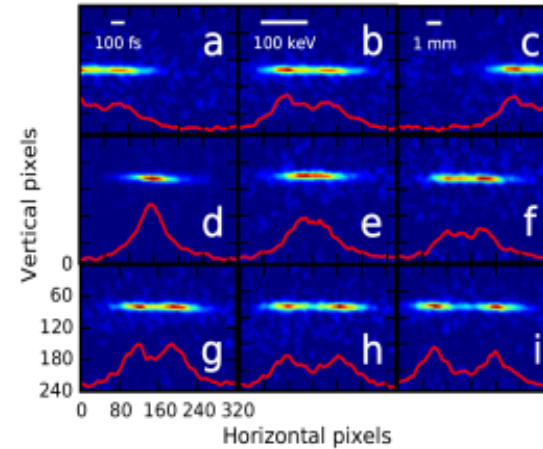
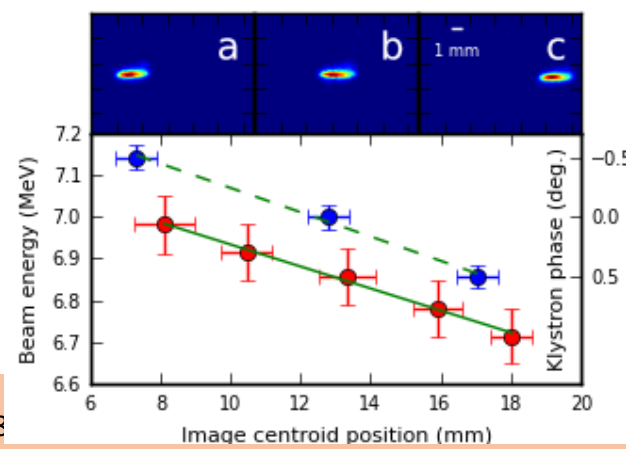
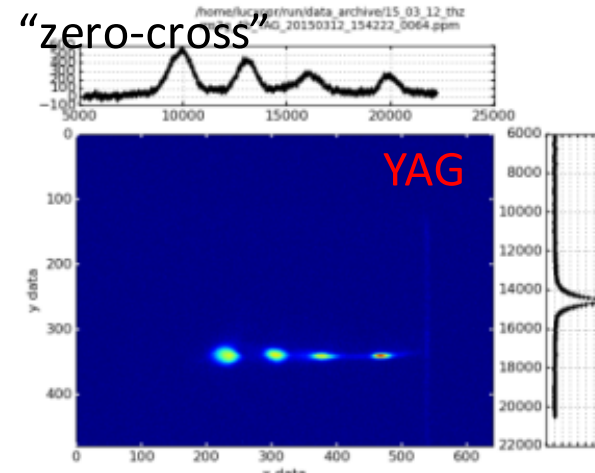
A. Aryshev, M. Shevelev, Y. Honda, N. Terunuma, J. Urakawa,
Femtosecond response time measurements of a Cs₂Te photocathode,
Appl. Phys. Lett. 111, 033508 (2017).

Measured Cs₂Te photocathode
peak-to-peak response time **369.48 ± 27 fs.**

“Kly1 off”

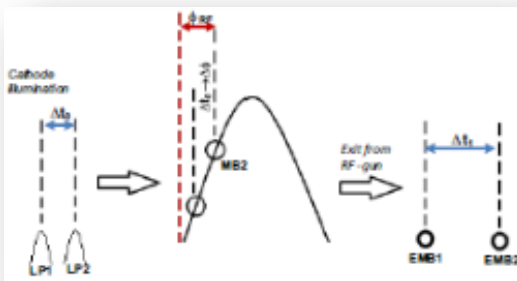


“zero-cross”

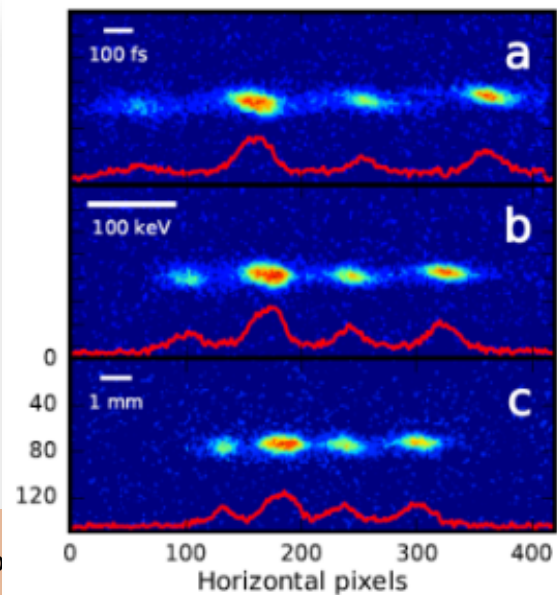


Tunability

“phase” modulation

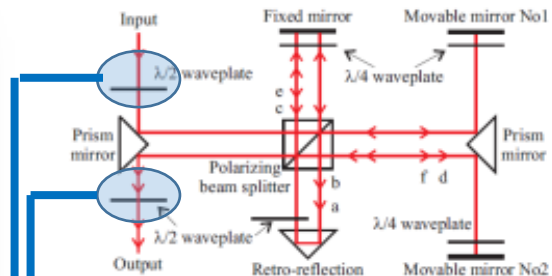


$$\Delta t = \Delta\phi / \omega_{rf}$$

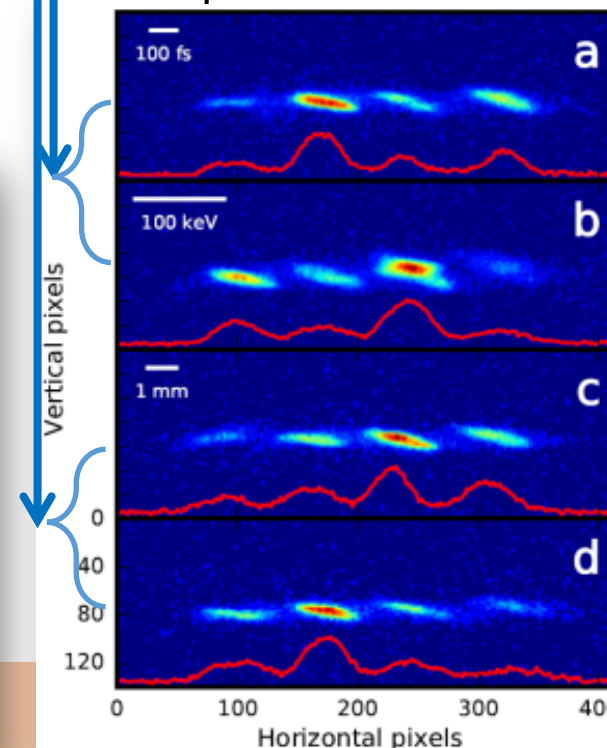


28 Sep

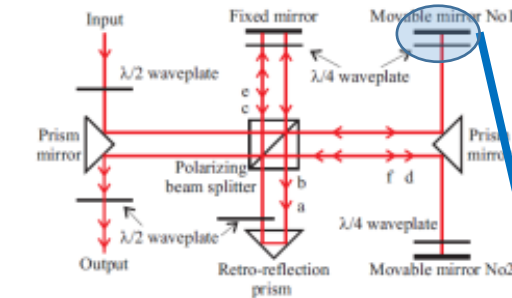
M. Shevelev, A. Aryshev, N. Terunuma, and J. Urakawa,
“Generation of a femtosecond electron microbunch train from
a photocathode using twofold Michelson interferometer”,
Phys. Rev. Accel. Beams **20**, 103401 (2017).



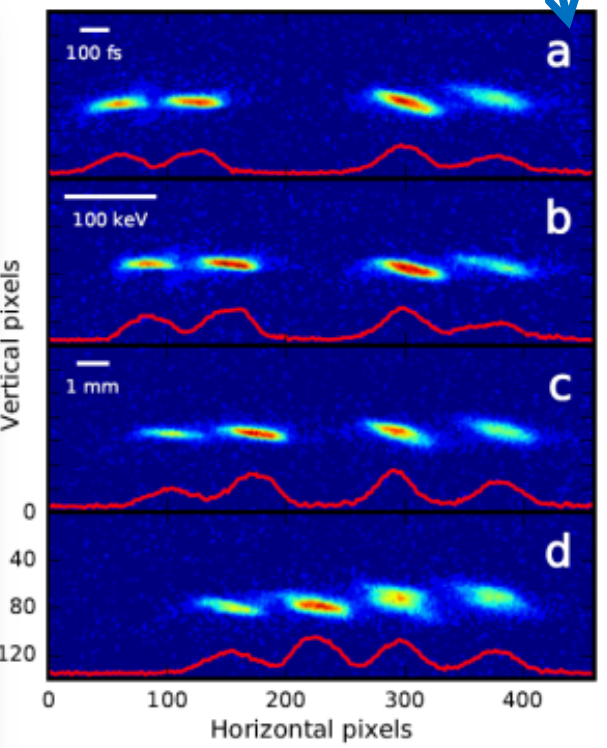
Amplitude modulation



28 Sep



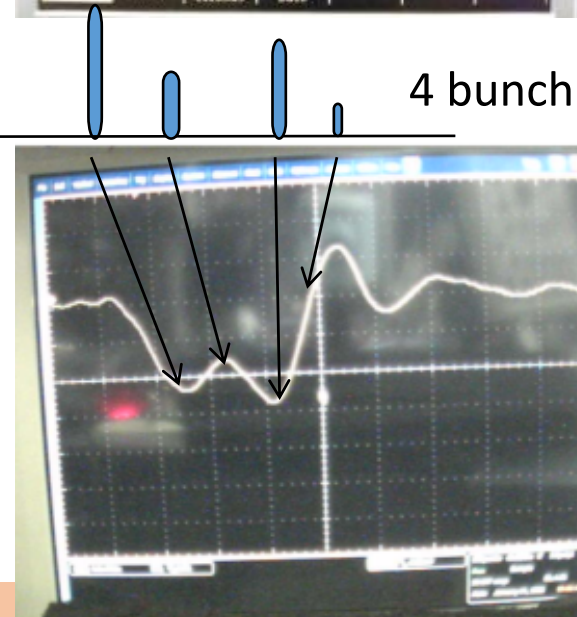
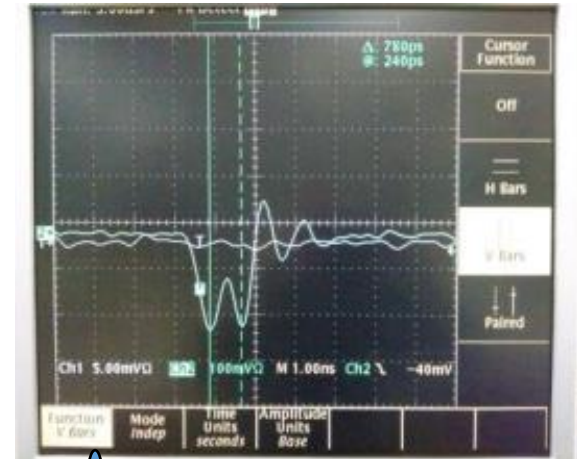
“phase” modulation



23

4-multi bunch generation

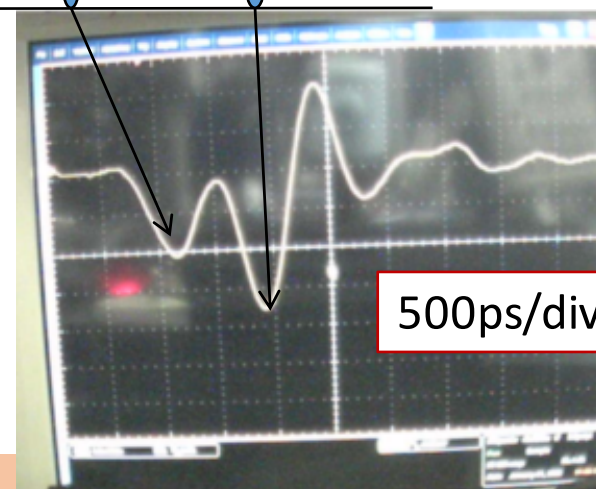
Tek TDC 684B, 1GHz, 5Gs/s



Tek DPO 7354, 5GHz, 40Gs/s



2 bunch



30m RF cable

Every second bucket (~700ps)



1m RF cable

Space-charge force suppression

I. Serafini, et.al. NIMA 387 (1997) 305-314

$$\Delta L_{sc} = \frac{4Qc}{I_A \gamma'^2 R^2} f(A, \gamma_f) \quad (6)$$

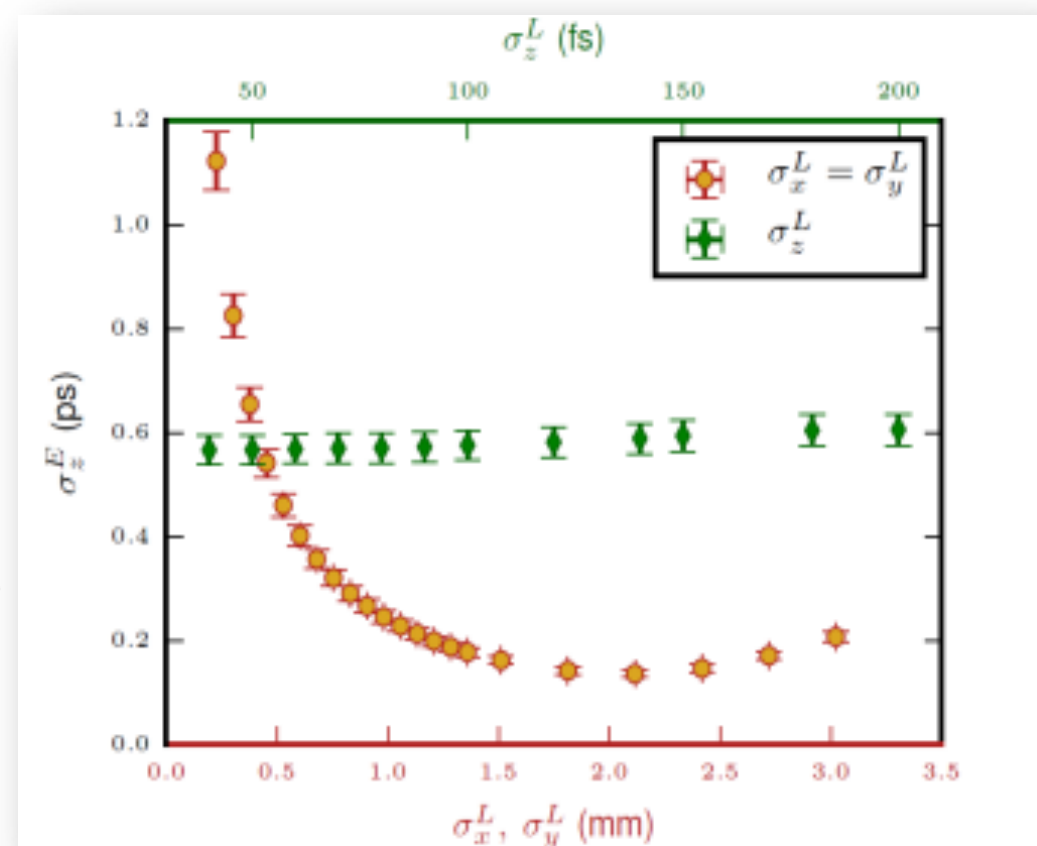
where I_A is the Alfvén current, Q the bunch charge, and

$$f(A, \gamma_f) = \left\{ \begin{array}{l} A(1 - 1/\gamma_f) + \sqrt{1 + A^2/\gamma_f^2} + (1 - A) \log \left[\frac{\gamma_f}{1 + \gamma_f} \right] \\ + A[\text{arc sinh}[A] - \text{arc sinh}[A/\gamma_f]] - \log[2](A - 1) \\ - \sqrt{1 + A^2} \\ \times \left(1 + \log \left[\frac{A^2(1 + \gamma_f)}{A^2 - \gamma_f + \sqrt{1 + A^2}\sqrt{1 + A^2/\gamma_f^2}} \right] \right) \end{array} \right\}$$

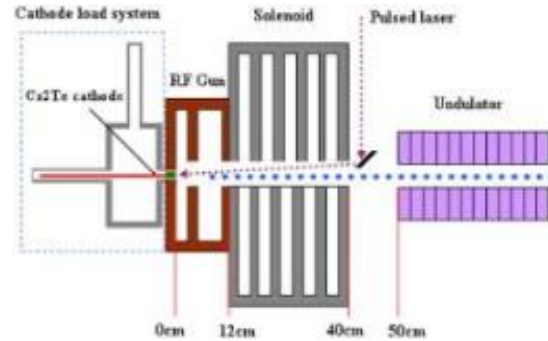
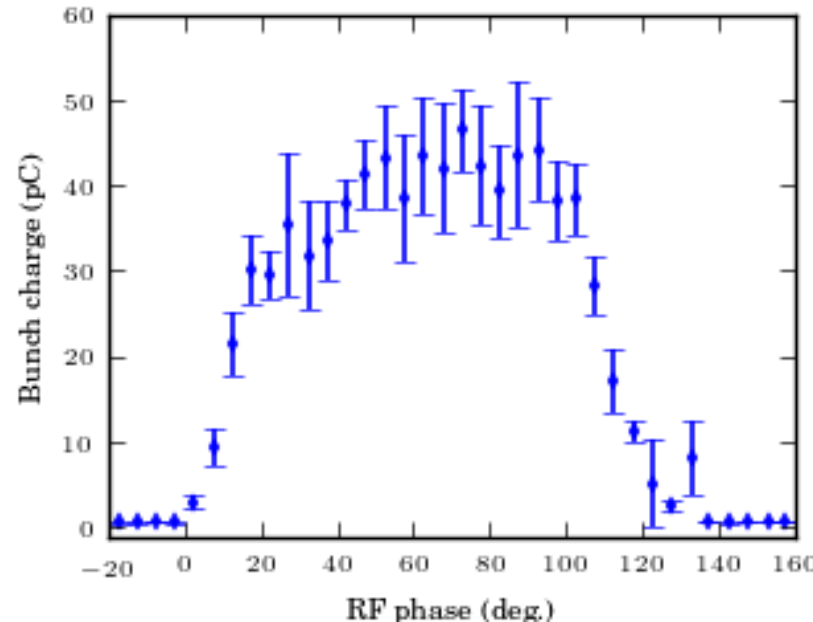
- Acceleration gradient, up \rightarrow limited by discharge
- Charge, down \rightarrow limited by detector's sensitivity
- UV spot size, up \rightarrow limited by off-axis dynamics
- UV Pulse length, !!! \rightarrow limited by THG
- Multi-bunch \rightarrow limited only by beam-loading

ASTRA simulation, LUCX RF gun

M. Shevelev, A. Aryshev, Y. Honda, N. Terunuma, J. Urakawa, Influence of space charge effect in femtosecond electron bunch on coherent transition radiation spectrum, Nucl. Instrum. Methods Phys. Res., Sec. B 402, 134 (2017).



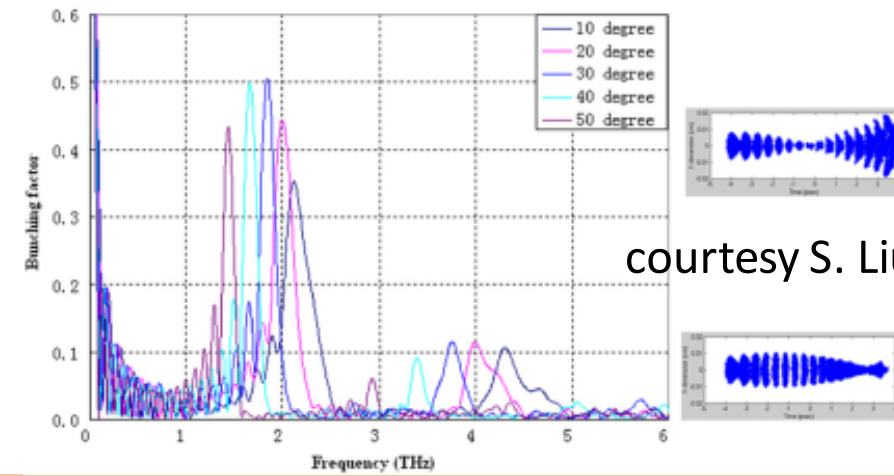
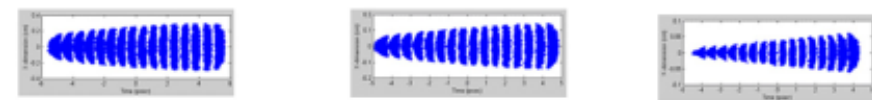
Number of micro-bunches/RF bucket ?



Parameters that will be naturally different for every micro-bunch:

- Charge (pow(N,2) dependence)
- E, dE (Linear dependence)
- Sigma_z (exponential dependence)
- Sigma_x,y (depends on radiation type)

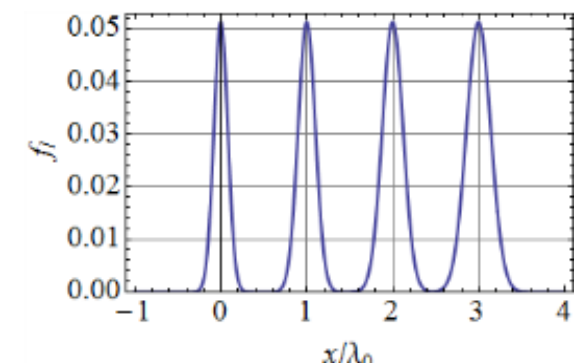
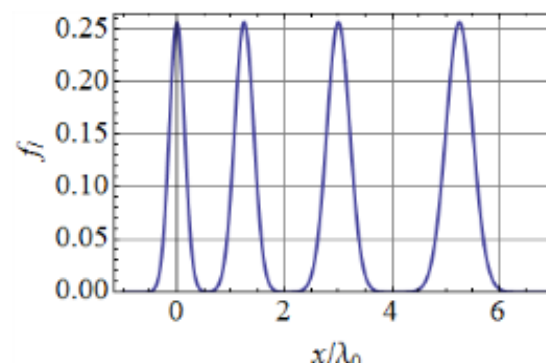
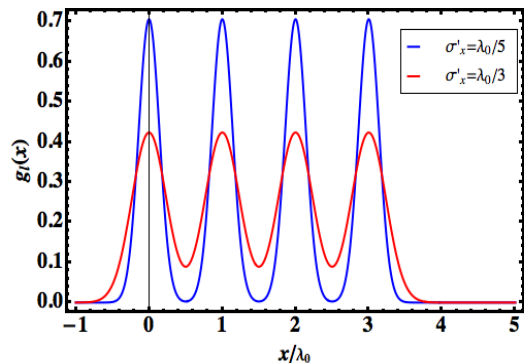
16 micro-bunch ASTRA simulation



courtesy S. Liu

Number of micro-bunches/RF bucket (work in progress)

$$f_l(x) = A \sum_{s=0}^{N_b-1} \exp\left[-\frac{(x-s\lambda_s)^2}{\sigma_s^2}\right], \quad \int_{-\infty}^{+\infty} dx f_l(x) = 1, \quad A = \left(\sqrt{\pi} \sum_{s=0}^{N_b-1} \sigma_s\right)^{-1}.$$



$$F = N F_{\text{inc}} + N(N-1) F_{\text{coh}},$$

$$F_{\text{inc}} = \int_V d^3r \left| e^{-i\mathbf{q}(\mathbf{r}-\mathbf{r}_0)} \right|^2 P(\mathbf{r}),$$

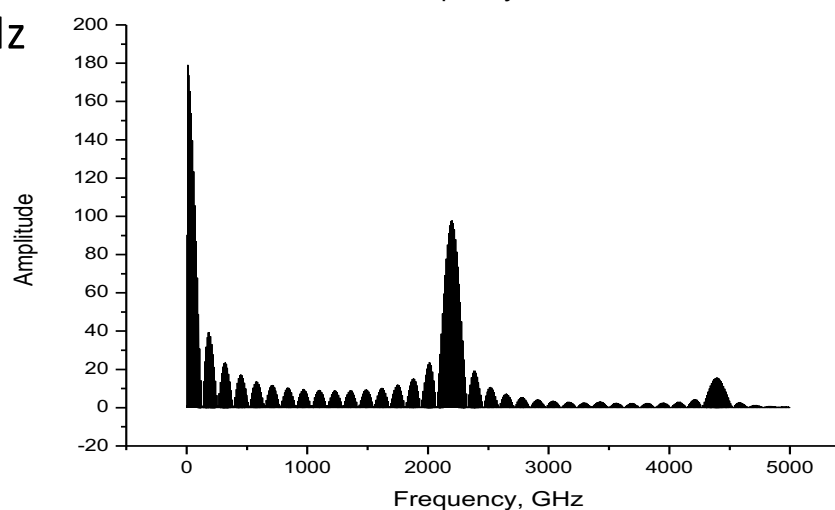
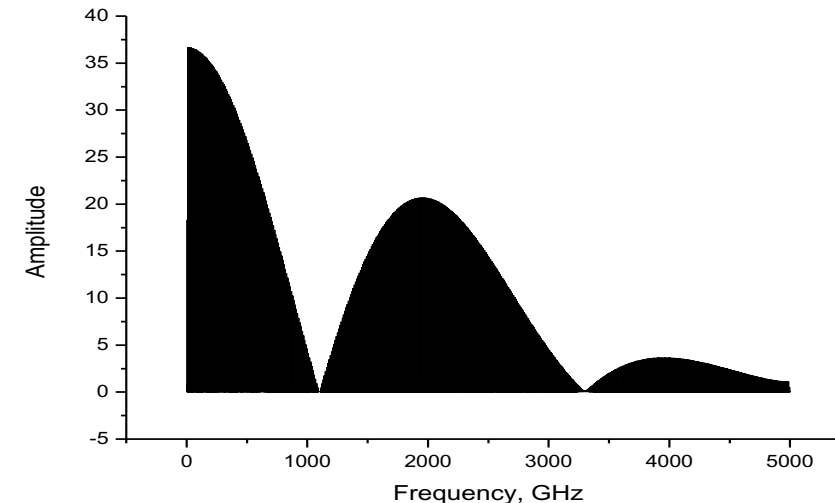
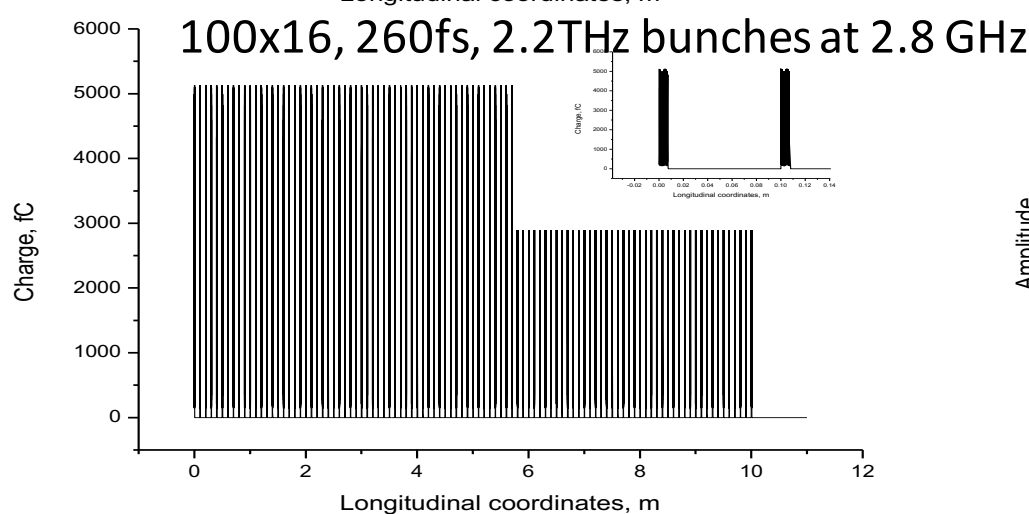
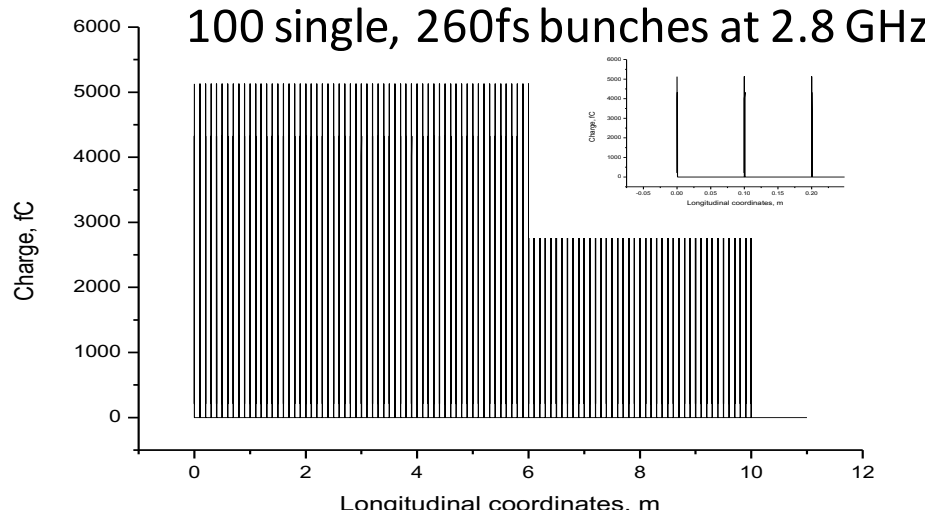
$$F_{\text{coh}} = \left| \int_V d^3r e^{-i\mathbf{q}(\mathbf{r}-\mathbf{r}_0)} P(\mathbf{r}) \right|^2,$$

$$F_{\text{coh}\parallel} = \left| \frac{\sum_{s=0}^{N_b-1} \sigma_s e^{-\frac{\omega}{c\beta} \left(\frac{\sigma_s^2}{4} \frac{\omega}{c\beta} + i s \lambda_s \right)}}{\sum_{s=0}^{N_b-1} \sigma_s} \right|^2.$$

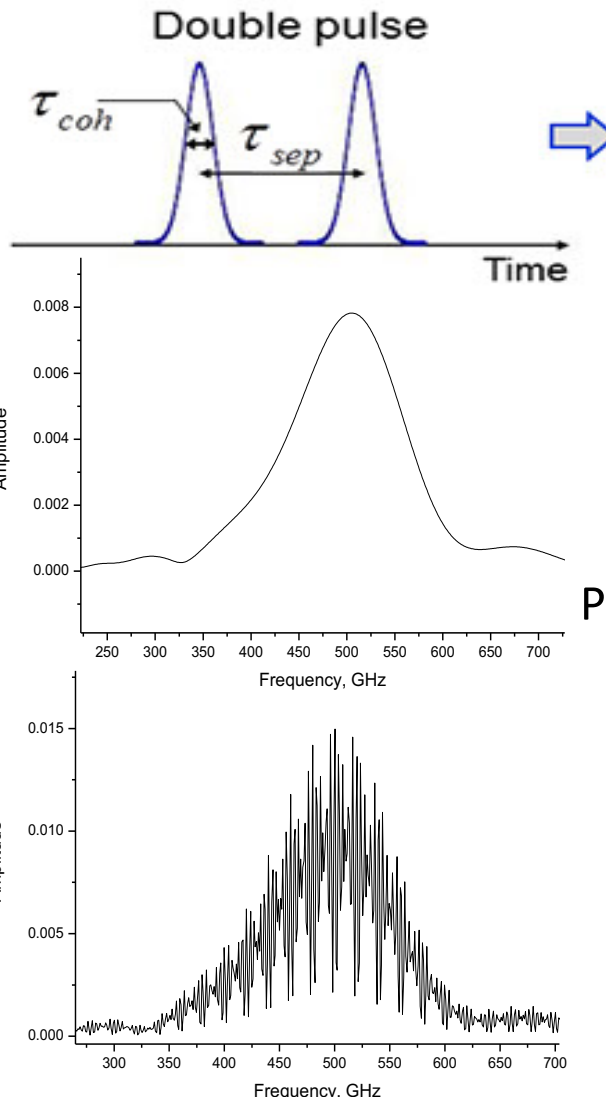
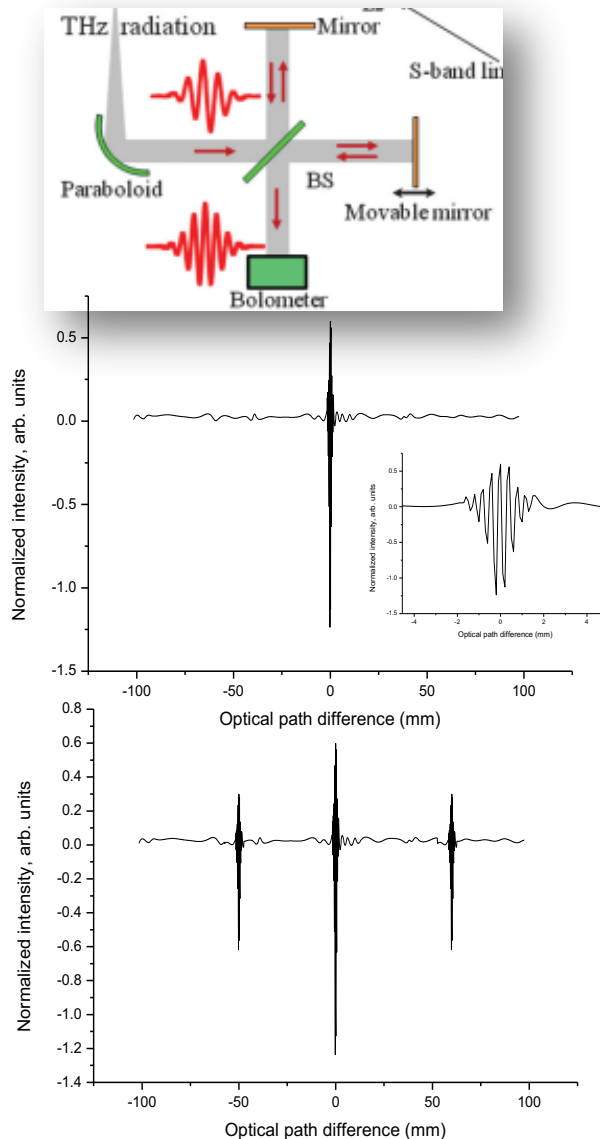
$$F_l = \exp\left[-\frac{\sigma_x^2 \xi^2}{2}\right] \frac{1}{N_b^2} \frac{\sin^2(N_b \lambda_0 \xi / 2)}{\sin^2(\lambda_0 \xi / 2)}, \quad \xi = \varphi / \nu.$$

- Amplitudes (charge)
- Function on phase

Longitudinal form-factor



Michelson interferometer as a direct time-domain analyzer

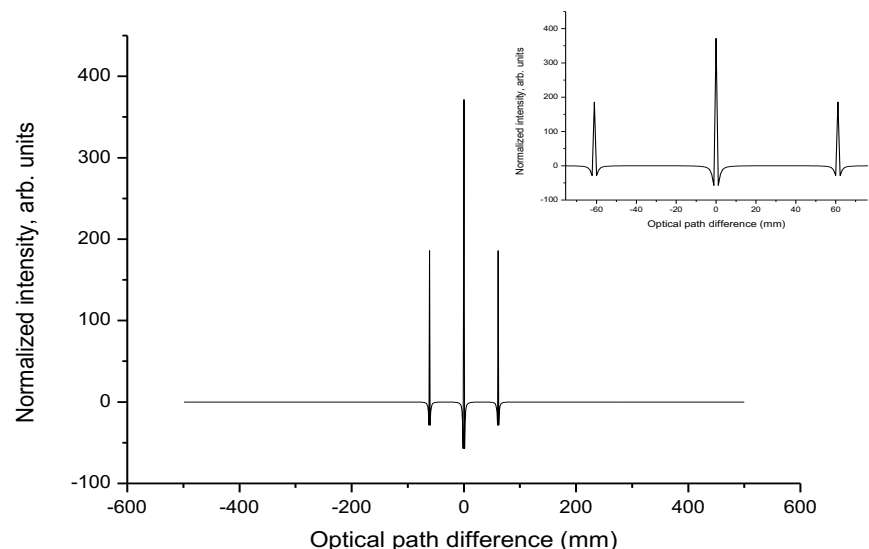
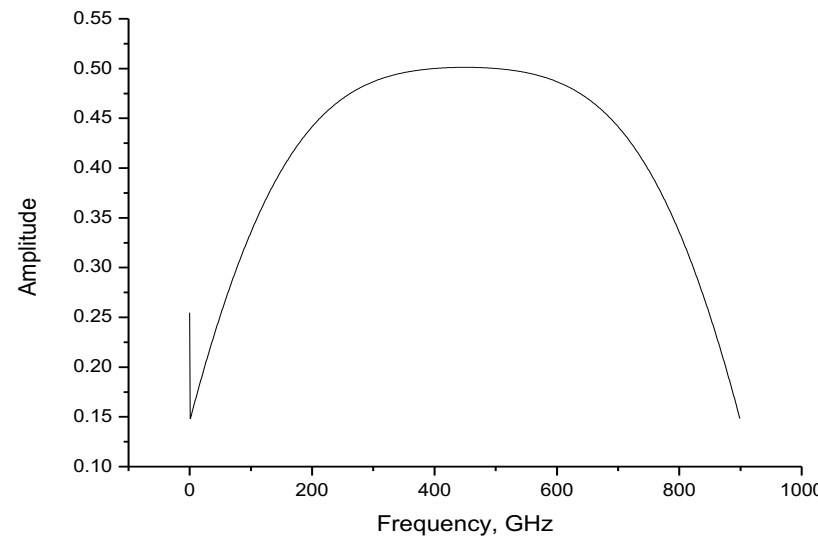
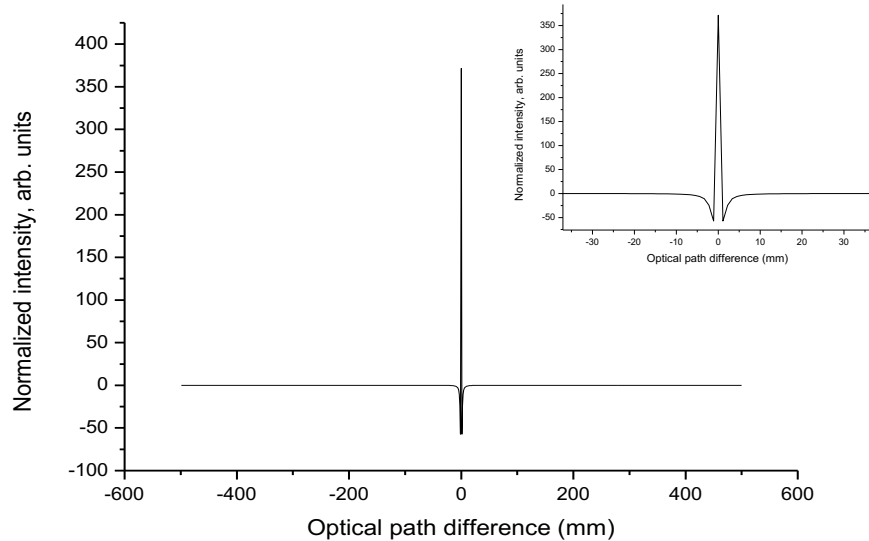


CTR – broadband spectrum
 SBD – narrowband sensitivity
 SBD speed \ll bunch separation

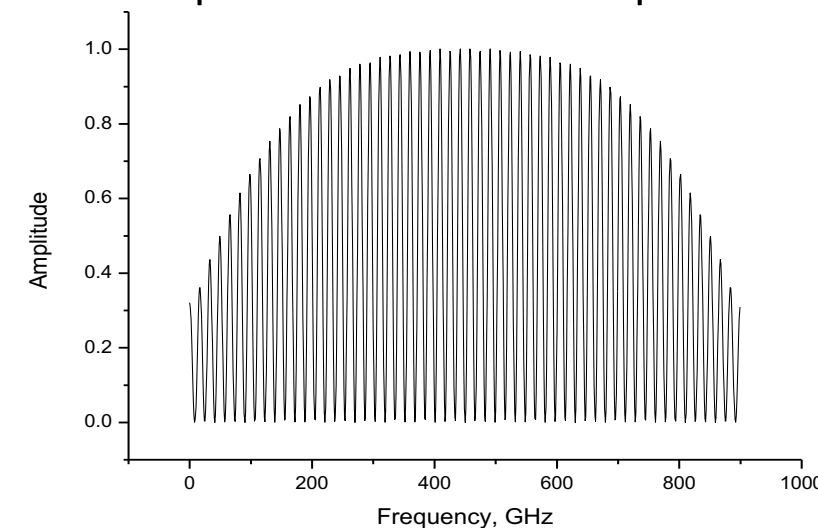
Pulse separation \gg radiation pulse duration

FT of two radiation pulses gives discrete spectra lines whereas each pulse has broad spectrum !!!

Michelson interferometer as a direct time-domain analyzer



Pulse separation >> radiation pulse duration

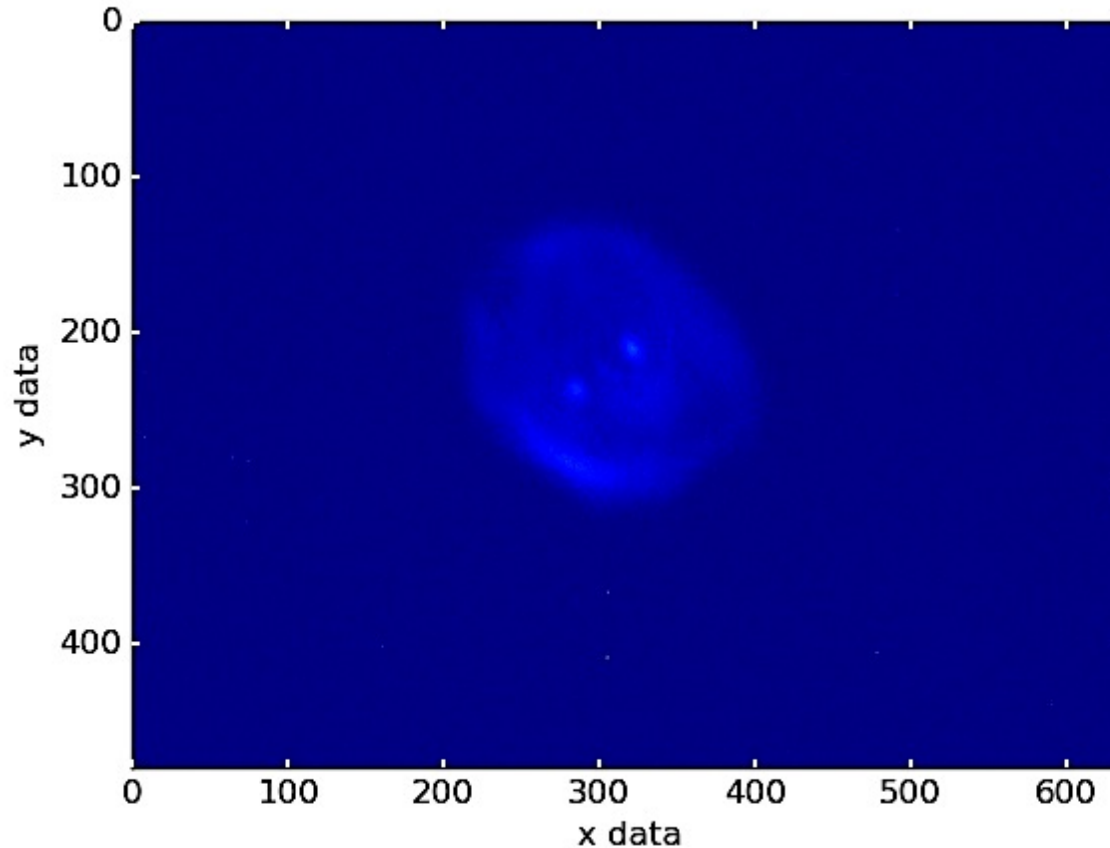


Conclusion & Summary

- Following electron beam parameters we confirmed:
 - Energy ~ 8.5 MeV
 - Energy spread < 1 % rms
 - Transverse rms beam size @ THz station ~ 500x500 um
 - Bunch length ~ 360 fs peak-to-peak (4 micro-bunch average)
 - Number of micro-bunches – 4
 - Minimum micro-bunch time separation ~ 0 fs
 - Micro-train charge (4 micro-bunches) ~ 0 - 200 pC
 - Bunch rep.rate THz+GHz+Hz was confirmed. Addition of MHz rep.rate require construction of the fiber laser system.

Conclusion & Summary

- A new concept of self-similar (fractal) beam is introduced.
- Direct utilization of THz+GHz e-beam is obvious for UR, cSPR, ChR.
- Care should be taken with short pulse processes like CTR and CDR.
- MHz repetition and associated radiation pulses can be trapped in the enhancement cavity.
- Michelson interferometer can be considered as a powerful tool for a direct time-domain measurements.
- Detector time response plays an important role.
- A care should be made in determination of the super-radiant radiation spectral characteristics.
- Near future demands include:
 - Effective longitudinal diagnostics (both laser pulses and e-beam).
 - Theoretical extension to account for realistic beam parameters.

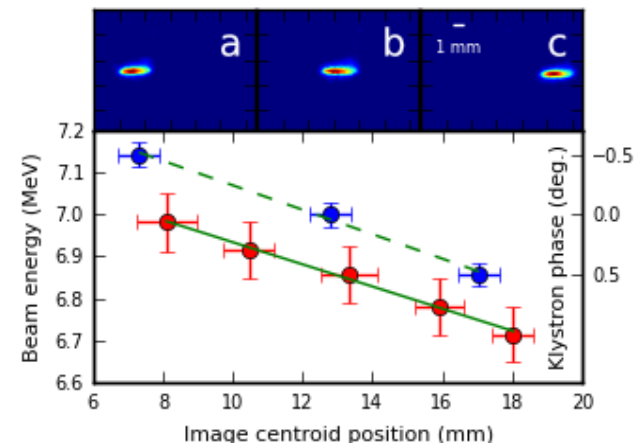


Thank you for your attention

Materials

- **Jean-Claude Diels, Wolfgang Rudolph:** “Ultrashort laser pulse phenomena”, Second edition, 2006
- **Tone Rotar,** “Ultrashort laser pulses”, Ms Thesis.
- **Carlo Antoncini,** “Ultrashort Laser Pulses”, Lecture notes.
- **Yuelin Li,** ANL, 2008 USPAS, summer session lecture notes.
- **Valerii (Vartan) Ter-Mikirtychev,** “Fundamentals of Fiber Lasers and Fiber Amplifiers”, Springer, 2014
- **Yan YOU,** “Yb-doped Mode-locked fiber laser based on NLPR”, 2012
- **Alexander Mikhailovsky,** “Basics of femtosecond laser spectroscopy”
- **Jeremy R. Gulley,** “Simulation of Ultrashort Laser Pulse Propagation and Plasma Generation in Nonlinear Media”.
- **S. LI et al.** PHYS. REV. ACCEL. BEAMS 20, 080704 (2017)
- **H. Tomizawa,** “Adaptiveaptive3D-Laser pulse shaping System to Minimize Emittance for Photocathode RF gun”, WEBAU01, FEL 2007

Miro-bunch train characterization



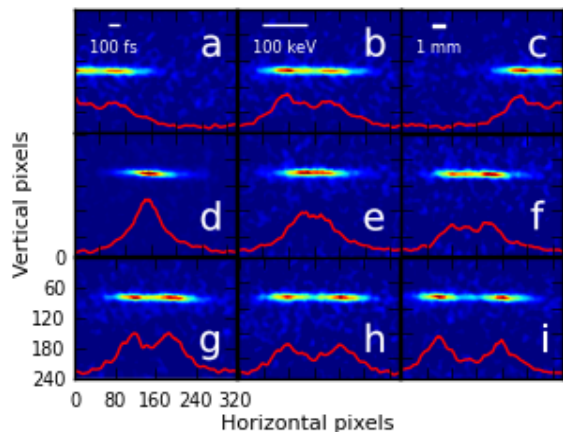
Top row: typical electron density distributions for different BH1G current.

Bottom: beam image centroid position vs electron beam energy (red dots) with linear fit:

$$\text{amplitude } 7.2 \pm 0.02 \text{ MeV}$$

$$\text{and slope } -2.65 \cdot 10^{-2} \pm 1.16 \cdot 10^{-3} \text{ MeV/mm}$$

Beam image centroid position vs RF phase (blue dots) with linear fit: slope $0.102 \pm 7.3 \cdot 10^{-3} \text{ deg./mm}$

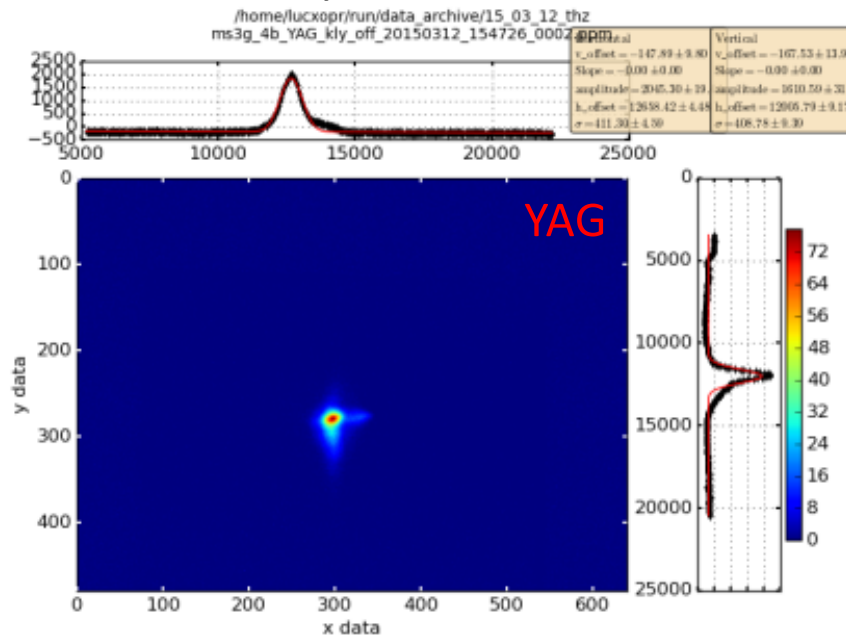


Typical electron density distribution measured for (a): -0.25 deg., (b): 0 deg., (c): 0.25 deg. accelerating phase;

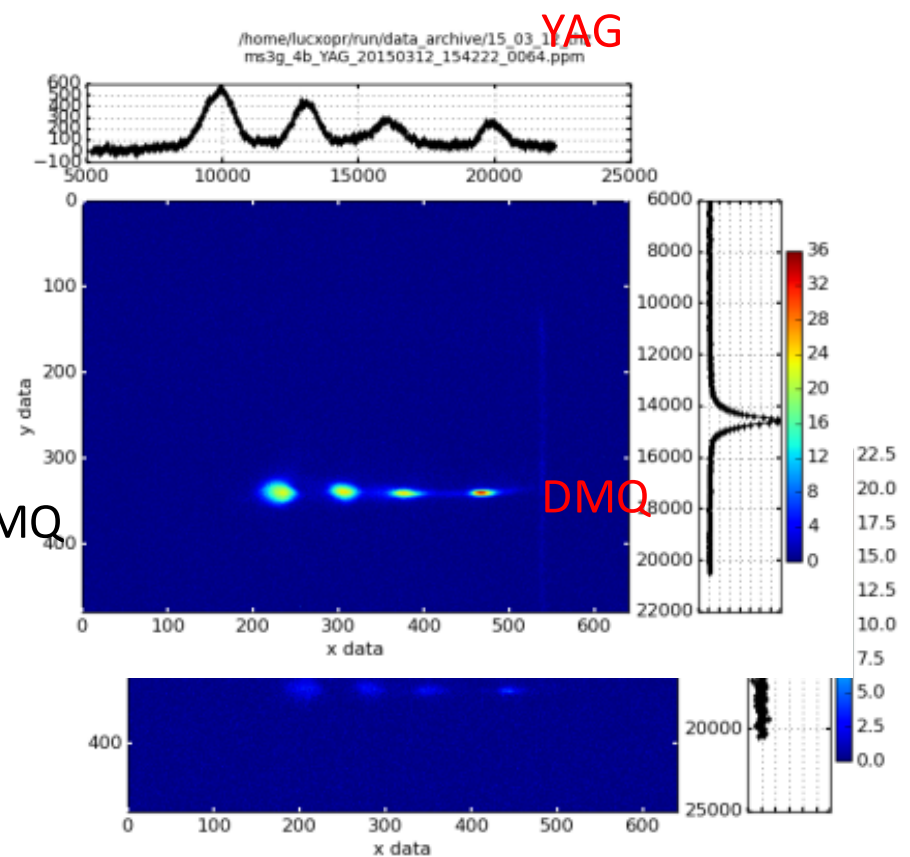
(d - i): Typical two micro-bunch electron density distribution measured for 0 deg. accelerating phase and (d): 4.8 mm, (e): 4.815 mm, (f): 4.825 mm, (g): 4.850 mm, (h): 4.865 mm, (i): 4.875 mm relative M2 mirror positions.

4-micro bunch generation

“Kly1 off”



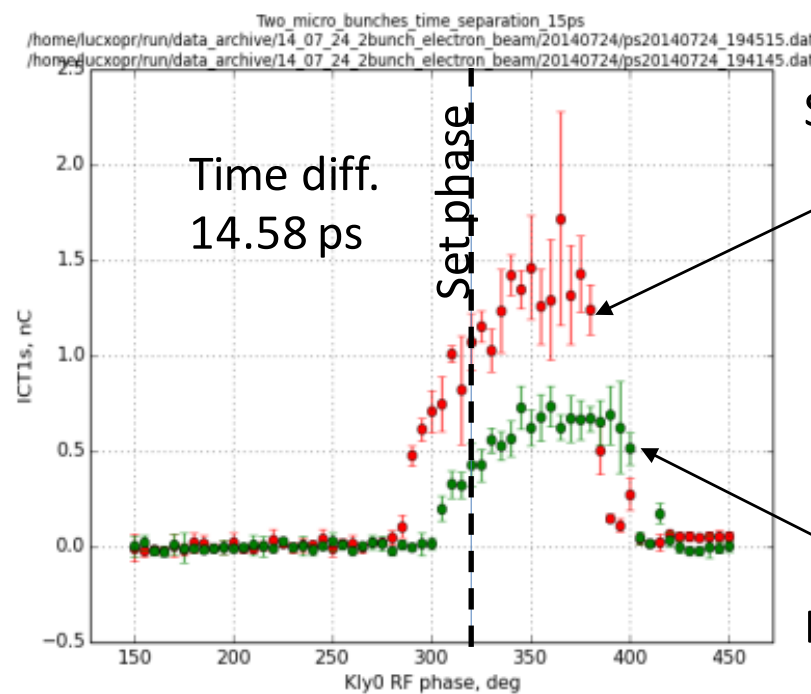
“zero-cross”



- YAG screen shows greater performance over DMC
 - Analysis should be improved
 - Beam dynamics and coherent radiation studies already can be performed

Initial two micro bunch observation

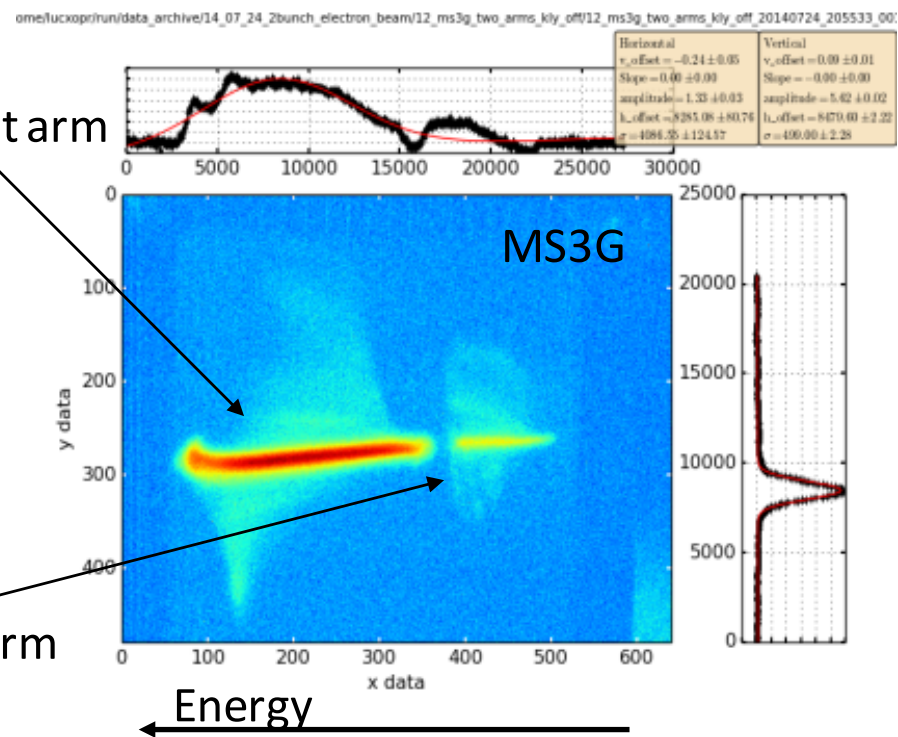
25/07/2014 Measured at high charge
due to limited ICT sensitivity



Straight arm

Bend arm

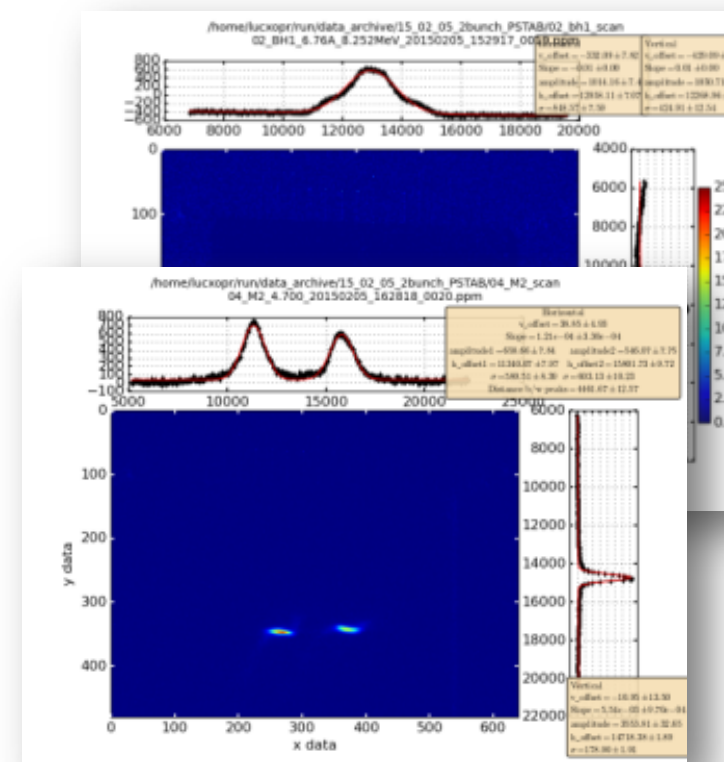
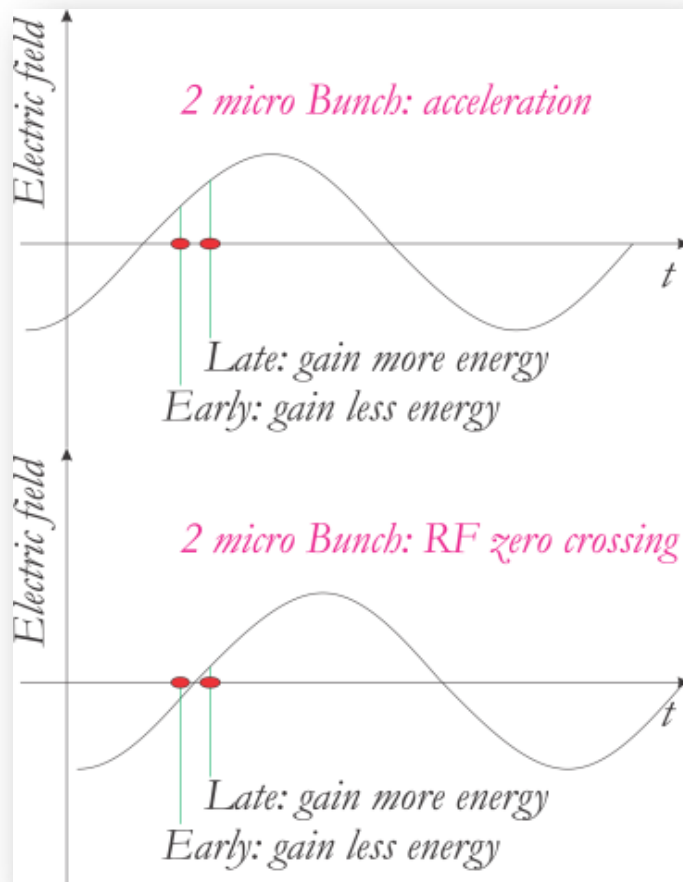
Ballistic e-optics, Klystron1 off



Set RF phase for both 320 deg.
Actual accelerating phase:
20 deg. – bend arm
35 deg. – straight arm

$$\begin{aligned} E_{\text{straight}} &= 8.70 \pm 0.003 \text{ MeV} \\ dE_{\text{straight}} &= 165.0 \pm 5.02 \text{ keV} \\ E_{\text{bend}} &= 8.34 \pm 0.003 \text{ MeV} \\ dE_{\text{bend}} &= 66.08 \pm 2.51 \text{ keV} \\ E_{\text{diff}} &= 360 \pm 4.2 \text{ keV} \end{aligned}$$

RF zero-crossing



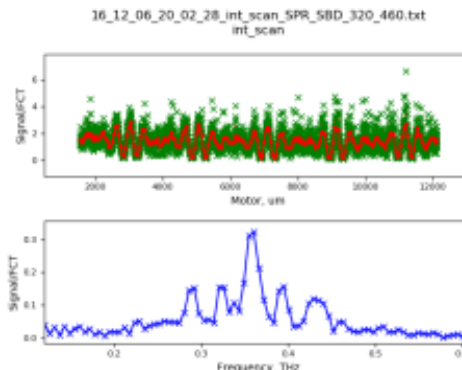
KEK-TPU, Super-radiant radiation emission study.

Summary of 2016.12.06 study

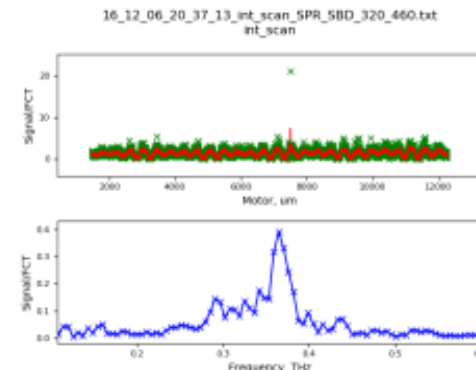
	CDR	cSPR	ASTRA
1 bunch	Int scan vs RF gun ϕ , 3 points	Int scan vs RF gun ϕ , 3 points	✓
2 bunch	M2 scans low and high Q	-	-
4 bunch	<ul style="list-style-type: none"> • M1 scan low and high Q • FSTB att scan • Int scan vs RF gun ϕ, 6 points 	<ul style="list-style-type: none"> • - • - • Int scan vs RF gun ϕ, 3 points 	✓ 6 points

cSPR

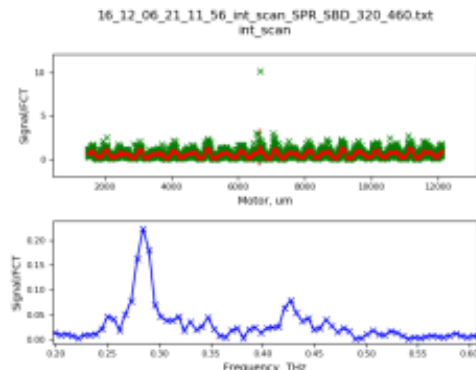
1 bunch



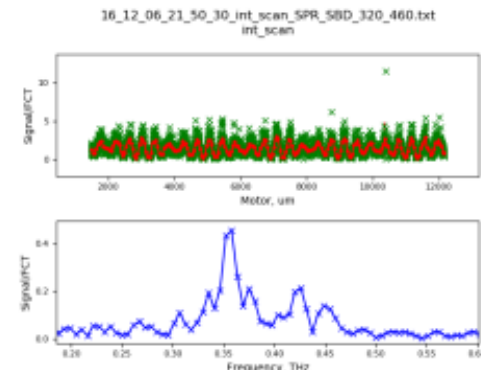
4 bunch



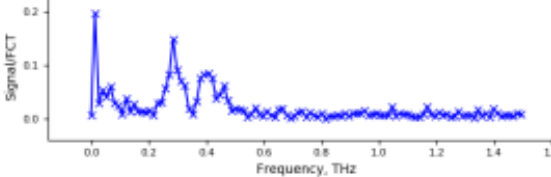
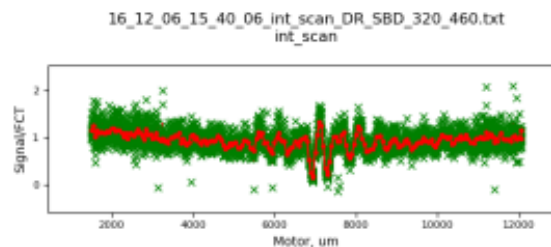
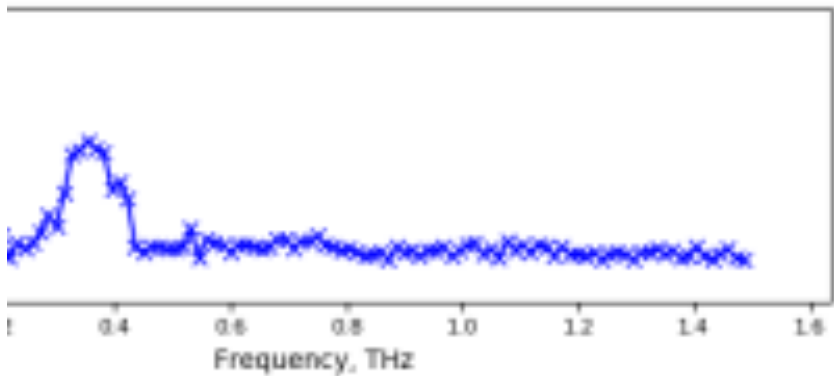
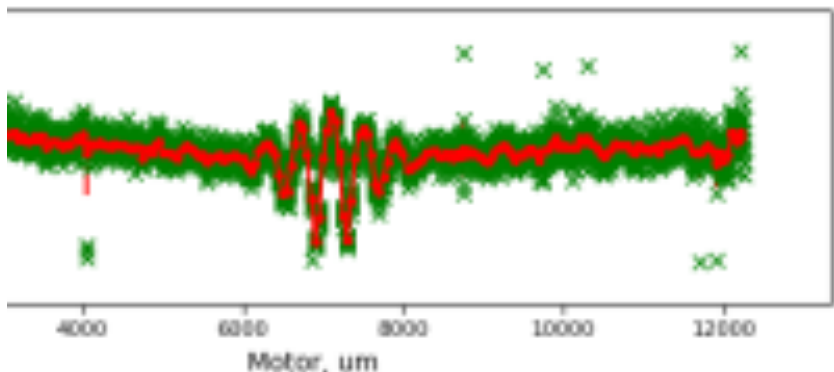
4 bunch



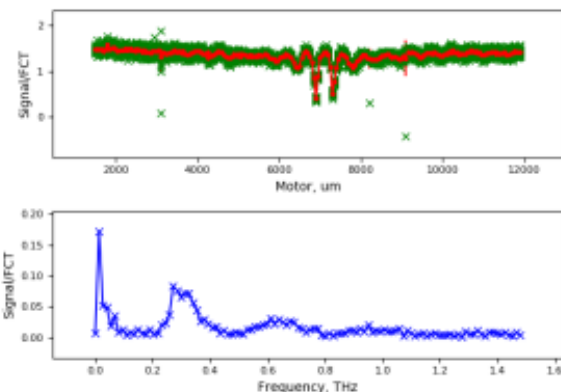
4 bunch



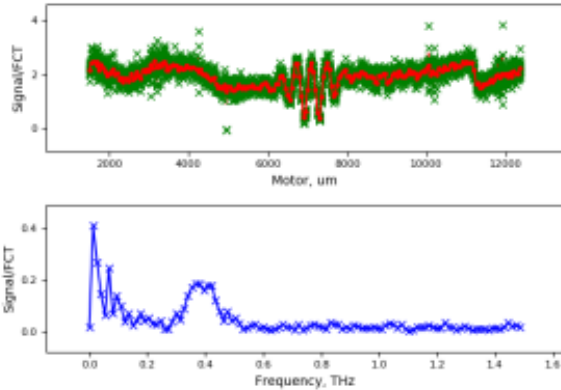
_06_14_03_52_int_scan_DR_SBD_320_460.txt
int_scan



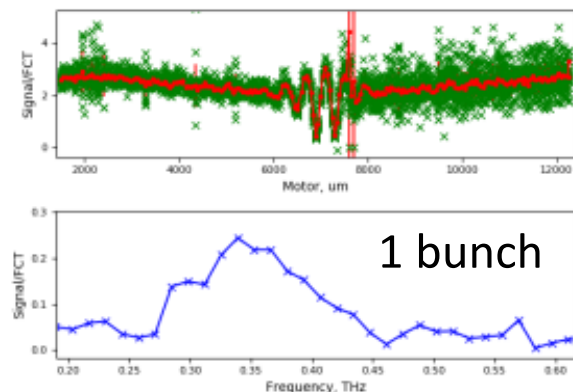
16_12_06_13_23_40_int_scan_DR_SBD_320_460.txt
int_scan



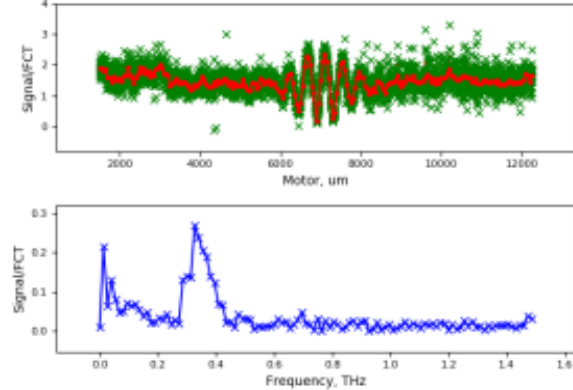
16_12_06_14_35_31_int_scan_DR_SBD_320_460.txt
int_scan



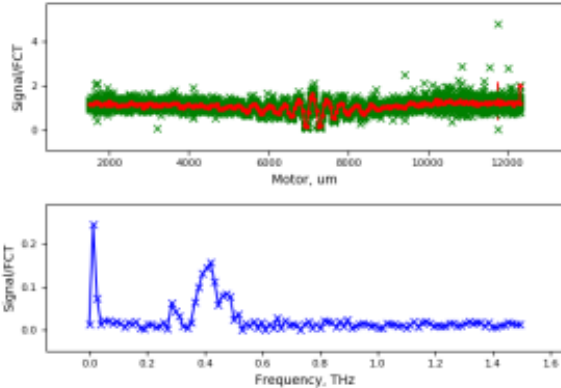
16_12_06_18_23_23_int_scan_DR_SBD_320_460.txt
int_scan



16_12_06_15_07_56_int_scan_DR_SBD_320_460.txt
int_scan



16_12_06_16_11_41_int_scan_DR_SBD_320_460.txt
int_scan



16_12_06_16_43_47_int_scan_DR_SBD_320_460.txt
int_scan

